







SASPARM

Support Action for Strengthening Palestinian-administrated Areas capabilities for seismic Risk Mitigation

Call ID FP7-INCO.2011-6.2

MODULE 3: GROUND RESPONSE ANALYSES AND NEAR-SURFACE SITE CHARACTERIZATION

Prof. Carlo G. Lai, PhD (carlo.lai@unipv.it)

in collaboration with

Dr. Laura Scandella, PhD Mr. Ali Guney Ozcebe, MSc GROUND RESPONSE ANALYSES

NNU, May 2 – 4, 2013













Outline

- One-dimensional ground response analyses
 - Motivation and examples of local ground amplification
 - Transfer function applied to ground response analysis
 - Linear and linear equivalent ground response analysis
 - Stochastic ground response analyses
- Model parameters for ground response analyses
 - Linear and linear-equivalent models
 - Non-linear models for 1D excitation and kinematics
 - Brief on fully non-linear models
- A brief introduction to 2D ground response analyses
 - Geometric scattering and topographic amplification
 - (De)-focalization, trapped waves and basin effects













Motivation











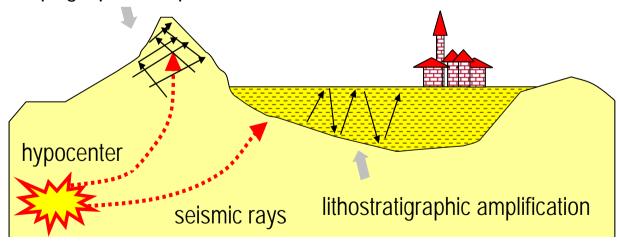


Statement of the problem

- Modifications of characteristics of ground motion caused by local geological-geomorphological-geotechnical conditions:
 - Lithostratigrafic amplification
 - Topographic amplification

local site effects

topographic amplification







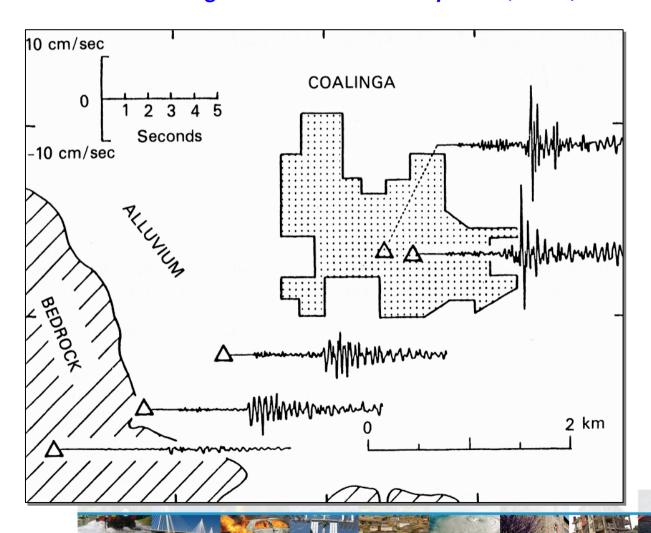








1983 Coalinga, California earthquake (M 4.3)













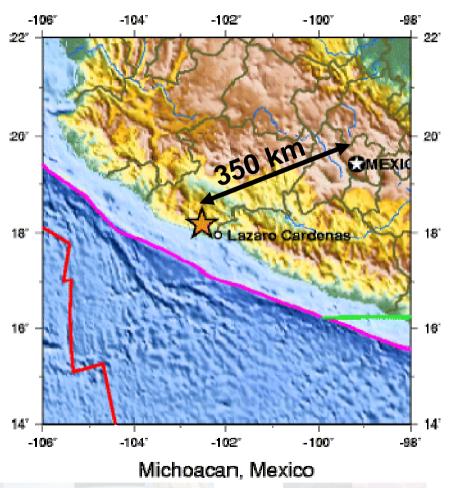


1985 Michoacan, Mexico earthquake (M_S 8.1)

EXAMPLE: MICHOACÀN Earthquake (M8.1) MEXICO CITY, SEPTEMBER 19, 1985



greater damage at 5 to 15 storey buildings despite <u>distance > 350 km</u> from ipocentre









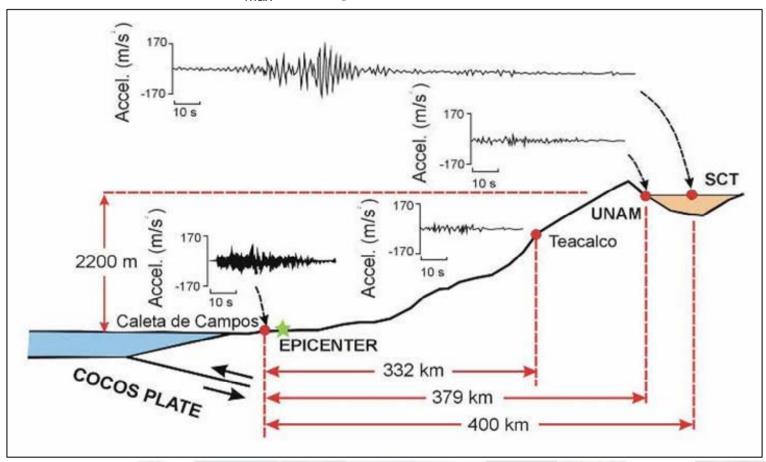






1985 Michoacan, Mexico earthquake (M_S 8.1)

On SCT seismic station a_{max} = 0.17 g







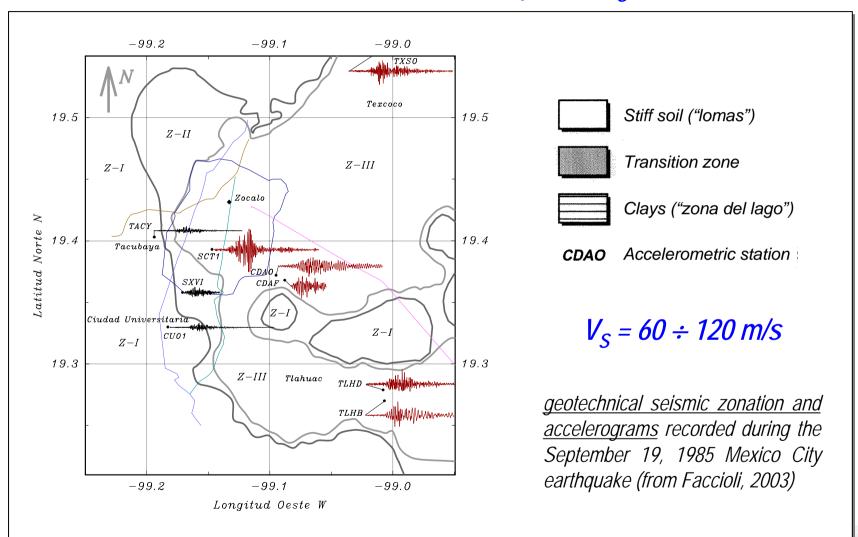








1985 Michoacan, Mexico earthquake (M_S 8.1)







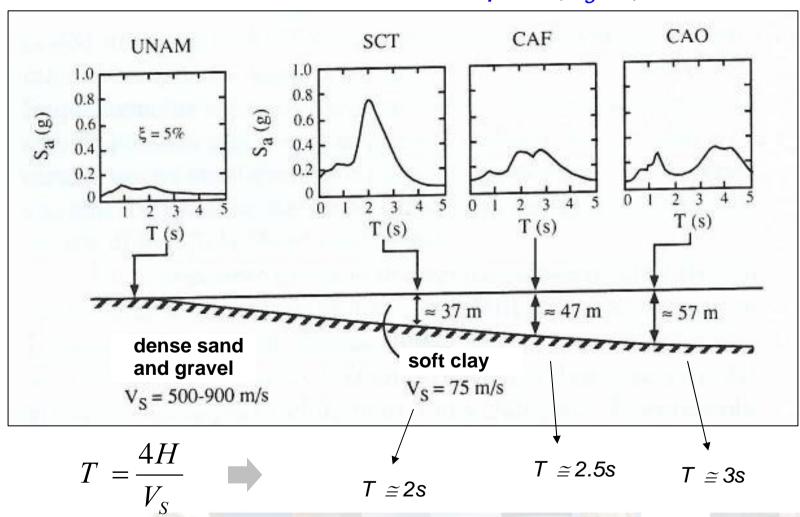








1985 Michoacan, Mexico earthquake (M_S 8.1)















1985 Michoacan, Mexico earthquake (M_S 8.1)

 v_s (m/s) 200 300 400 Geotechnical seismic zonation of the Mexico City area 500 600 Stiff soil ("lomas") 19.50 Transition zone Clays ("zona del lago") Accelerometric station Depth (m) 19.40 TACY SCT CDAO SCT D is the zone that 40 CUIP suffered the most damage 19.30 severe TLHD during the 1985 TLHB: Michoacan event CDAO 60 -99.20 -99.10 -99.00











1963 Skopje, Macedonia earthquake (M_W 6.1)



anomalous ground amplification due to 2D geological configuration

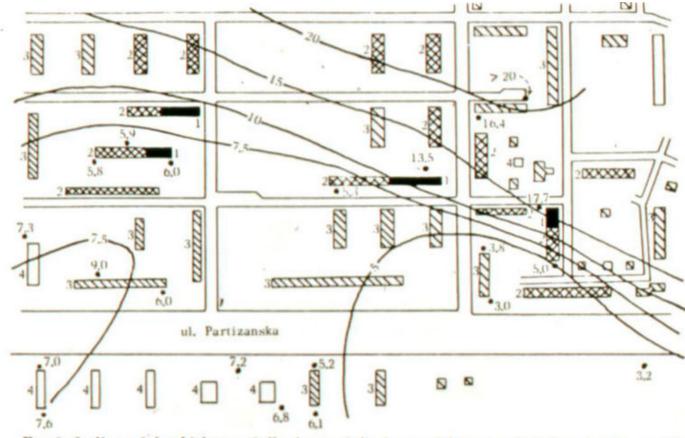


Fig. 8. Isolines of the thickness of alluvium and the degree of damage to buildings in "Karposh" (western part of the city). Isolines are in meters. Notation for the degree of damage is the same as in Figure 7. Note that all of the destroyed buildings (but one) are on the belt of abrupt change in the alluvium thickness.















1963 Skopje, Macedonia earthquake (M_W 6.1)

Geological cross section of the town of Skopje

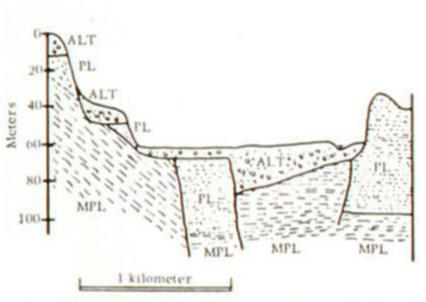


Fig. 4. Cross section through the city (see Figure 2, section B-B). ALT is alluvium terrace (gravel with sand); PL is Pliocene (sand and gravel with clay, conglomerates, marl); MPL is Mio-Pliocene (mostly marl).















1963 Skopje, Macedonia earthquake (M_W 6.1)

Geological cross sections corresponding to most damaged areas

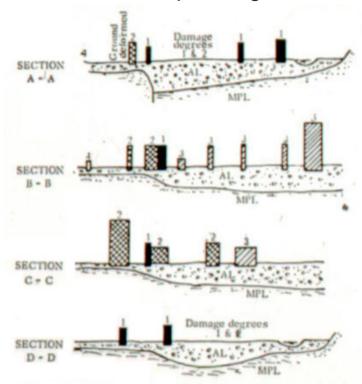


Fig. 7. Cross section through the most heavily damaged regions (see Figure 2, sections A-A to D-D). Degrees of damage: 1—destroyed, 2—heavy damaged, 3—little damaged, 4—slightly damaged. Al—alluvium, MPL—Mio-Pliocene. Note the sharp change in the thickness of the alluvium on the left side of each section.









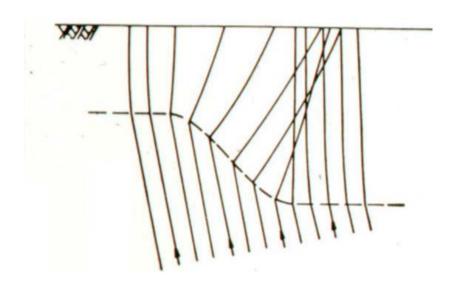


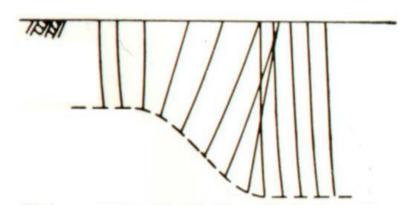




1963 Skopje, Macedonia earthquake (M_W 6.1)

Geometric interpretation of ground amplification at the town of Skopje





Focusing by the fault (P waves)

Focusing by the fault (SV waves)





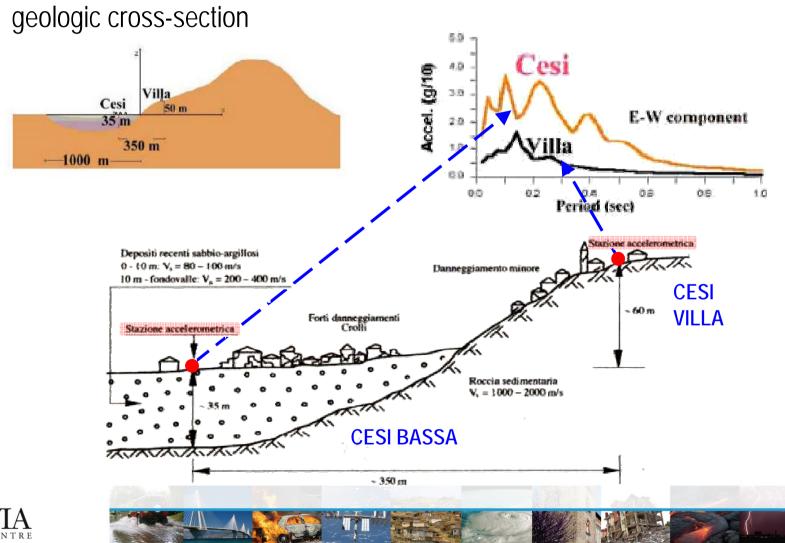








1997 Umbria-Marche (Italy) earthquake (M 5.9)













Stationary response of a layer over the half-space











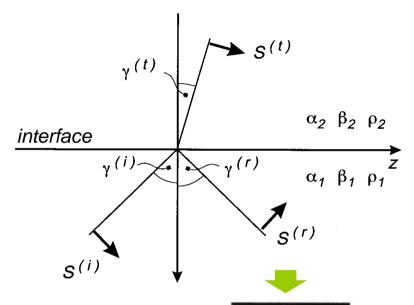


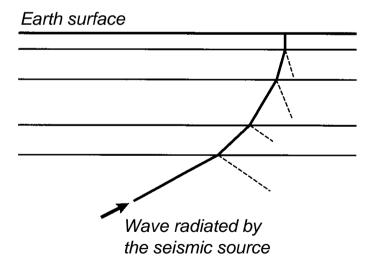
ONE-DIMENSIONAL GROUND RESPONSE ANALYSES

SNELL LAW

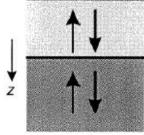
$$\frac{sin\,\gamma^{(i)}}{\beta_1} = \frac{sin\,\gamma^{(r)}}{\beta_1} = \frac{sin\,\gamma^{(t)}}{\beta_2}$$







vertical propagation of waves in plane and parallel soil profiles with impedance contrast from bottom to top (1D site effect)



1-1D

Trajectory of a seismic ray

1D -1D ground response analysis













ELASTIC LAYER OVER A RIGID HALF-SPACE

At the free-surface, the displacement of an arbitrary point of the half-space in case of a plane, incident harmonic wave is given by the superposition of u_i and u_r:

$$f\left(t + \frac{x}{c}\right) \qquad \qquad \downarrow f\left(t - \frac{x}{c}\right) \qquad \qquad \chi$$

$$u(x,t) = u^{i} + u^{r} = f\left(t + \frac{x}{c}\right) + f\left(t - \frac{x}{c}\right)$$
 free surface effect.

If harmonic waves:

$$u = \exp\left[i\omega\left(t + \frac{x}{c}\right)\right] + \exp\left[i\omega\left(t - \frac{x}{c}\right)\right] = 2\exp(i\omega t)\cos(Kx) \qquad (K = \omega/c) \qquad \text{where}$$

$$Re[u] = 2cos(\omega t)cos(Kx)$$

doubling of the amplitude caused by total reflection at the free surface

half-space oscillates in stationary state of vibration for any value of frequency of the incident wave





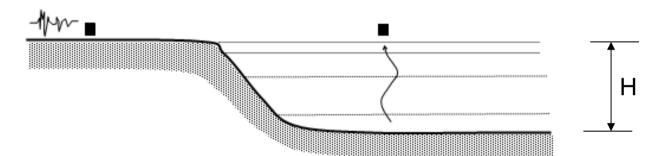








If the semi-infinite domain is replaced by a layer of thickness H resting over a RIGID BASE, the former undergoes stationary vibrations only if u(H) = 0, namely if:



$$\Rightarrow u = 2 \exp(i\omega t) \cos(Kx) = 0$$
 $\cos(KH) = 0$



$$cos(KH) = 0$$

from which

$$\omega_n = \left(n + \frac{1}{2}\right) \frac{\pi c}{H}, \quad or \quad f_n = \left(n + \frac{1}{2}\right) \frac{c}{2H} \quad (n = 0, 1, \dots) \qquad n = 0 \implies T = \frac{4H}{c}$$

$$n = 0 \implies T = \frac{4H}{c}$$

eigenvalues of the problem with boundary conditions:

1)
$$\sigma_x = (\lambda + 2\mu) \, \varepsilon_x = (\lambda + 2\mu) \, \frac{\partial u}{\partial x} = 0$$
 2) $\cos(KH) = 0$

$$2) \cos(KH) = 0$$











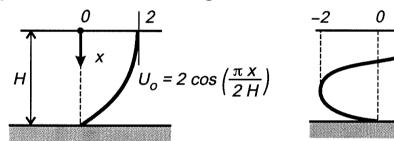


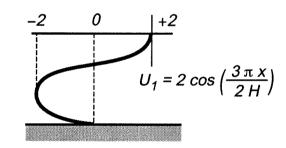
Corresponding "modes of vibrations" are obtained by replacing the eigenvalues in:

$$u = \exp\left[i\omega\left(t + \frac{x}{c}\right)\right] + \exp\left[i\omega\left(t - \frac{x}{c}\right)\right] = 2\exp(i\omega t)\cos(Kx)$$

and omitting the time harmonic dependence, obtaining:

$$\begin{cases} U_0 = 2\cos\left(\omega_0 \frac{x}{c}\right) = 2\cos\left(\frac{\pi x}{2H}\right) \\ U_1 = 2\cos\left(\omega_1 \frac{x}{c}\right) = 2\cos\left(\frac{3\pi x}{2H}\right) \end{cases}$$





first and second mode of vibration of the stratum

$$U_i = \dots$$

It should be noted that to U_0 is associated the wavelength λ_0 = 4H, to U_1 the wavelength λ_1 = (3/2)H, etc. Furthermore for $\omega = \omega_n$ it is always u(H)=0 and thus the amplitude ratio u(0)/u(H) becomes infinite.













If a sinusoidal motion of unit amplitude $e^{i\Omega t}$ is applied to the rigid base, the response of the elastic layer (which is a linear system) will also be sinusoidal with a frequency ω equal to the excitation frequency Ω .

In general, this response can be expressed as a sum of two waveforms propagating in two opposite directions with amplitudes A and B to be determined:

$$\mathbf{u} = \mathbf{A} \exp \left[\mathbf{i} \Omega \left(\mathbf{t} + \frac{\mathbf{x}}{\mathbf{c}} \right) \right] + \mathbf{B} \exp \left[\mathbf{i} \Omega \left(\mathbf{t} - \frac{\mathbf{x}}{\mathbf{c}} \right) \right]$$

From the free surface boundary condition it follows immediately that A = B, and thus:

$$u(x,t) = 2A\cos\left(\frac{\Omega x}{c}\right)\exp(i\Omega t) \tag{1}$$

For x = H, the displacement must be equal to the one prescribed, namely:

$$u(H, t) = 2A \cos\left(\frac{\Omega H}{c}\right) \exp(i\Omega t) = \exp(i\Omega t)$$













from which $A = \left[2\cos(\Omega H/c)\right]^{-1}$ and substituting in (1):

$$u(x,t) = \frac{\cos\left(\frac{\Omega x}{c}\right)}{\cos\left(\frac{\Omega H}{c}\right)} \exp(i\Omega t) \quad \text{which for } x = 0$$

$$u(0,t) = \exp(i \Omega t)/\cos(\Omega H/c) = u(H,t)/\cos(\Omega H/c)$$

Ratio:

$$\frac{u(0)}{u(H)} = \frac{1}{\cos\left(\frac{\Omega H}{c}\right)} = H_1(\Omega)$$
 transfer function of a layer over a rigid base

blows-up ($\rightarrow \infty$) for $\Omega = \omega_n$ (resonance!)





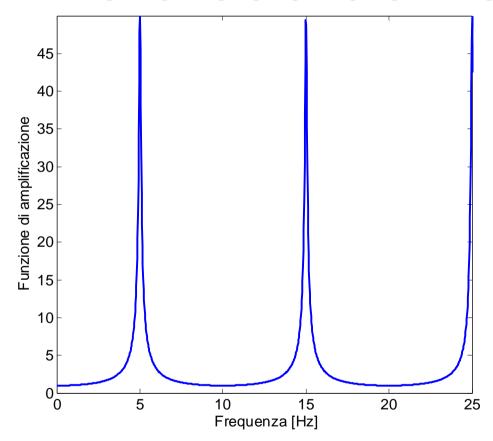


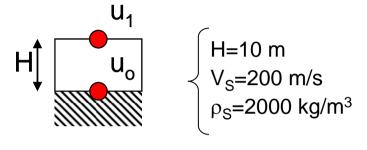






AMPLIFICATION FUNCTION FOR S-WAVES





$$\left| \frac{u(0)}{u(H)} \right| = \left| \frac{1}{\cos\left(\frac{\Omega H}{c}\right)} \right| = \left| H_1(\Omega) \right|$$

amplification function



$$n = 0 \implies T = \frac{4H}{V_S} = 0.2s \implies f = 5Hz$$













VISCOELASTIC LAYER OVER A RIGID HALF-SPACE

Elastic-viscoelastic correspondence principle:

Get
$$\frac{u(0)}{u(H)} = \frac{1}{\cos\left(\frac{\Omega H}{c^*}\right)} = H_1(\Omega)$$
 transfer function of a viscoelastic layer over a rigid bedrock

where
$$c^*(\omega) = \frac{c(\omega)}{\sqrt{[1+4D^2(\omega)]}} \cdot \left[\frac{1+\sqrt{[1+4D^2(\omega)]}}{2} + i \cdot D \right]$$

 $D(\omega)$ material damping ratio (in shear and compression)







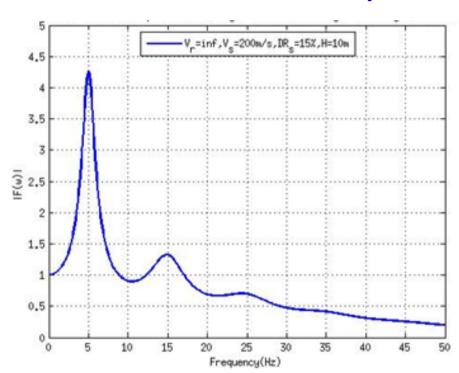


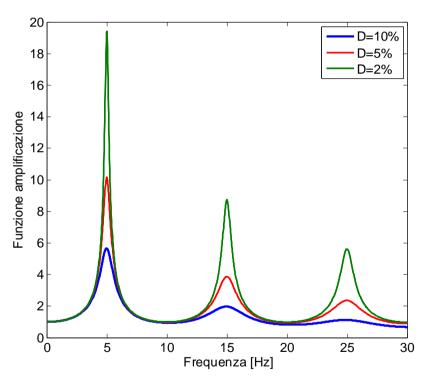




VISCOELASTIC LAYER OVER A RIGID HALF-SPACE

Amplification function





Effect of damping increases as frequency increases!





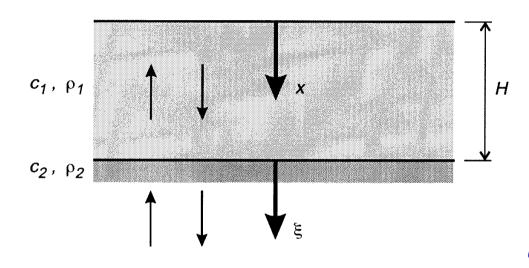








ELASTIC LAYER OVER AN ELASTIC HALF-SPACE



continuity of stress and displacement

$$\begin{cases} u_1(H,t) = u_2(0,t) \\ \rho_1 c_1^2 \frac{\partial u_1(H,t)}{\partial x} = \rho_2 c_2^2 \frac{\partial u_2(0,t)}{\partial \xi} \\ & \uparrow \end{cases}$$
can be P or S waves can be P or S waves

get
$$H_1(\omega) = \frac{u_1(0,t)}{u_1(H,t)} = \frac{1}{\cos\left(\frac{\omega H}{c_1}\right)}$$

like the case of a <u>rigid base</u>!





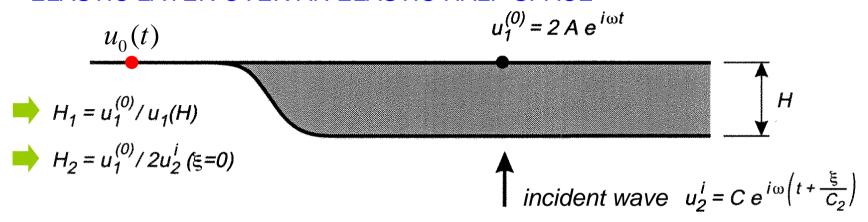








ELASTIC LAYER OVER AN ELASTIC HALF-SPACE



For any ω , the ratio between the displacement at the free surface of the layer and that of the <u>outcropping half-space</u> is:

$$H_{2}(\omega) = \frac{u_{1}(0,t)}{u_{0}(t)} = \frac{1}{\cos\left(\frac{\omega H}{c_{1}}\right) + i\frac{1}{\eta}\sin\left(\frac{\omega H}{c_{1}}\right)}$$

transfer function of the layer with respect to elastic base

where
$$\frac{1}{\eta} = \frac{\rho_2 c_2}{\rho_1 c_1}$$









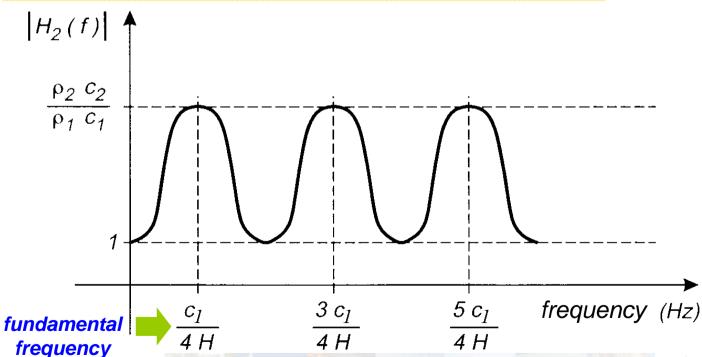




ELASTIC LAYER OVER AN ELASTIC HALF-SPACE

Get
$$A_2(f) = |H_2(f)| = \frac{1}{\left[\cos^2\left(2\pi f \frac{H}{c_1}\right) + \left(\frac{\rho_1 c_1}{\rho_2 c_2}\right)^2 \sin^2\left(2\pi f \frac{H}{c_1}\right)\right]^{\frac{1}{2}}}$$

amplification function of an elastic layer over an elastic bedrock









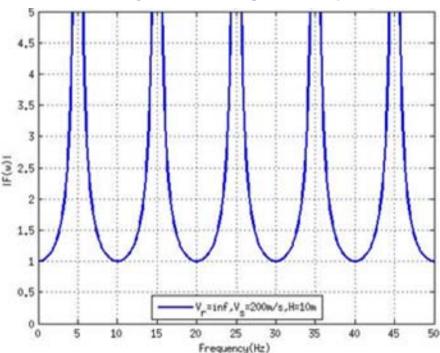




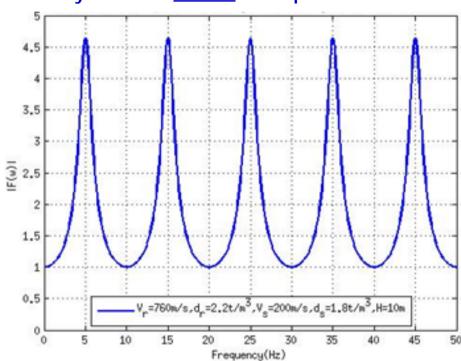


ELASTIC LAYER OVER AN ELASTIC HALF-SPACE

Amplification function of a single elastic layer over a <u>rigid</u> half-space



Amplification function of a single elastic layer over a <u>elastic</u> half-space



The presence of a <u>rigid</u> bedrock means that waves propagating downward into the soil are totally reflected towards the surface from the bedrock, trapping the elastic energy in the soil layer.













VISCOELASTIC LAYER OVER A VISCOELASTIC HALF-SPACE

Elastic-viscoelastic correspondence principle:

Get
$$H_2(\omega) = \frac{u_1(0,t)}{u_0(t)} = \frac{1}{\cos\left(\frac{\omega H}{c_1^*}\right) + i\frac{\rho_2 c_2^*}{\rho_1 c_1^*}\sin\left(\frac{\omega H}{c_1^*}\right)}$$
 transfer function of a viscoelastic layer over a viscoelastic bedrock

where
$$c_{\chi}^{*}(\omega) = \frac{c_{\chi}(\omega)}{\sqrt{[1+4D_{\chi}^{2}(\omega)]}} \cdot \left[\frac{1+\sqrt{[1+4D_{\chi}^{2}(\omega)]}}{2} + i \cdot D_{\chi}\right]$$
 $\chi = 1, 2$

with $D_{\gamma}(\omega)$ material damping ratio (in shear and compression)





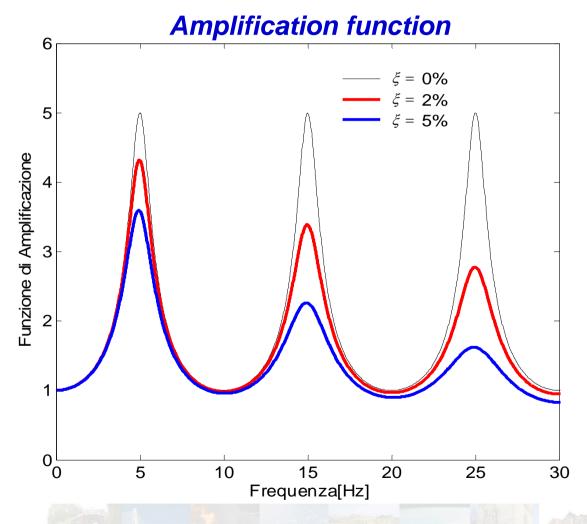








• VISCOELASTIC LAYER OVER A VISCOELASTIC HALF-SPACE













• VISCOELASTIC LAYERED PROFILE OVER A VISCOELASTIC HALF-SPACE

Layer	Coordinate	Properties	Thickness
	u_1		
1	z_1 u_2	$G_{l} $	h_1
2			· · · · · · · · · · · · · · · · · · ·
	z ₂ ▼		
•	u_m	•	
m	z_m	$G_m \stackrel{\xi}{\downarrow}_m P_m$	h_m
	u_{m+1}	6	
m+1	z_{m+1} u_{m+2}	$G_{m+1} \ \xi_{m+1} \ P_{m+1}$	h_{m+1}
m+2			•
•	z_{m+2}		
•	u_N	•	
N	z_N	$G_N \stackrel{\xi}{\varsigma}_N P_N$	$h_N = \infty$













VISCOELASTIC LAYERED PROFILE OVER A VISCOELASTIC HALF-SPACE

The relationship between the waves which propagate in adjacent layers is obtained by imposing the CONTINUITY between the <u>stress</u> and <u>displacement</u> at the interface between the two layers:

$$\begin{cases}
\tau_m(z_m = h_m, t) = \tau_{m+1}(z_{m+1} = 0, t) \\
u_m(z_m = h_m, t) = u_{m+1}(z_{m+1} = 0, t)
\end{cases}$$

$$u_{j}(z_{j},t) = A_{j}e^{i\omega\left(t + \frac{z_{j}}{\beta_{j}^{*}}\right)} + B_{j}e^{i\omega\left(t - \frac{z_{j}}{\beta_{j}^{*}}\right)}$$







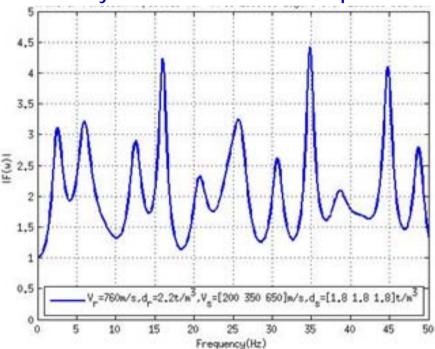




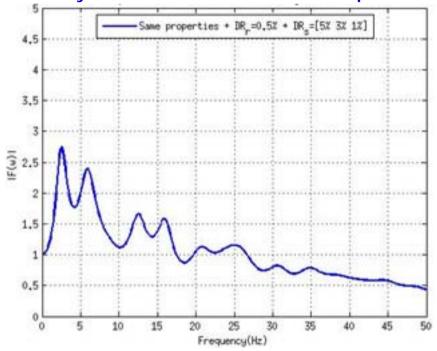


• VISCOELASTIC LAYERED PROFILE OVER A VISCOELASTIC HALF-SPACE

Amplification function of N elastic layers over an elastic half-space



Amplification function of N viscoelastic layers over a viscoelastic half-space















Linear and linear equivalent 1D ground response analysis













Linear equivalent 1D ground response analysis

SEISMIC EFFECTS DUE TO 1D GROUND AMPLIFICATION

1D ground response due to <u>vertical propagation of shear waves</u> in soil deposits constituted by a stack of plane and parallel layers with contrast of mechanical impedance from bottom to top.

\sim	<u> </u>
Layer 1	$h_1, \rho_1, V_{P1}, V_{S1}, D_{P1}, D_{S1}$
Layer 2	$h_2, \rho_2, V_{p_2}, V_{s_2}, D_{p_2}, D_{s_2}$
:	: : : : :
Layer n ₁	$h_{n_1}, \rho_{n_1}, V_{pn_1}, V_{sn_1}, D_{pn_1}, D_{sn}$





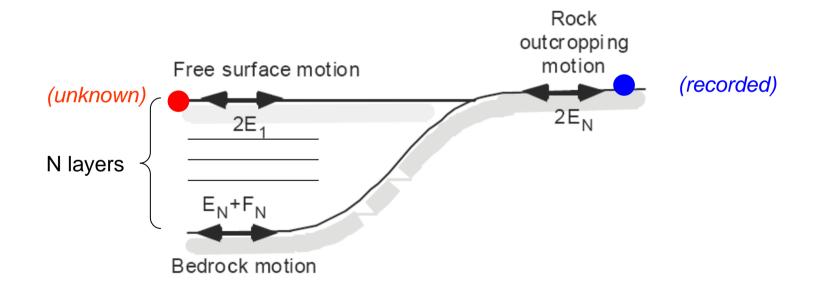




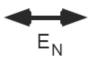




SCOPE: compute ground motion at the free surface of a soil deposit by knowing the ground motion at the outcropping bedrock



Incoming motion



(from EERA, 2001)







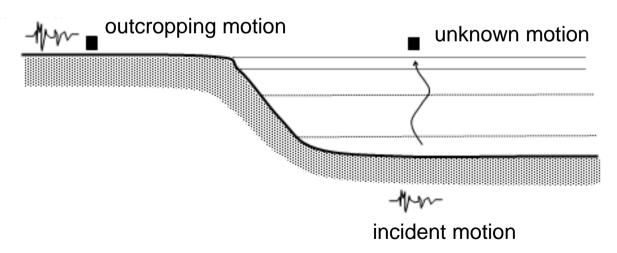






NEED TO DEFINE:

- 1. Geometric and kinematic idealization of the problem (e.g. 1D-1D)
- 2. Constitutive model of the subsoil (e.g. linear-equivalent elastic)
- 3. Seismic input (e.g. outcropping, within)
- 4. Algorithm and procedure of analysis (e.g. time vs. frequency)







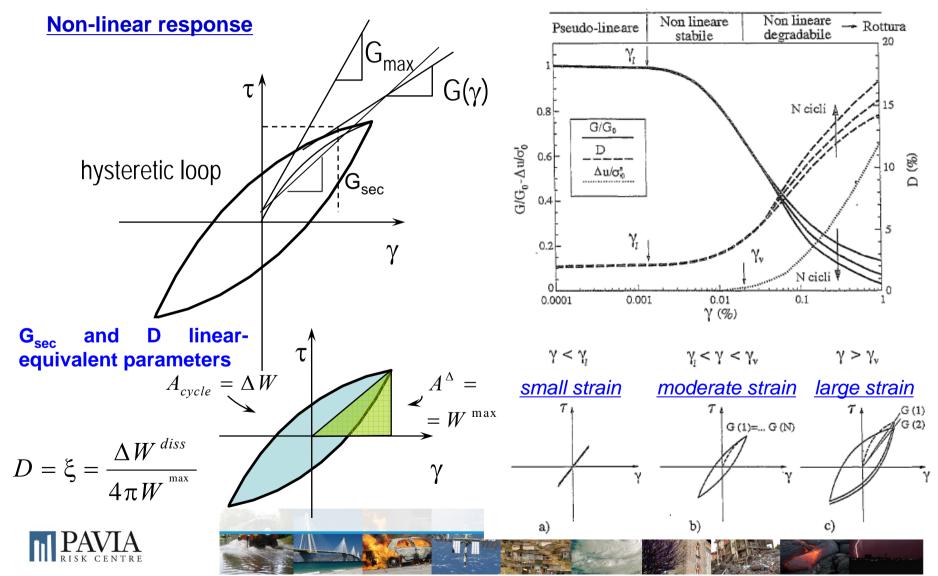








• FACTS OF SOIL RESPONSE UNDER CYCLIC LOADING





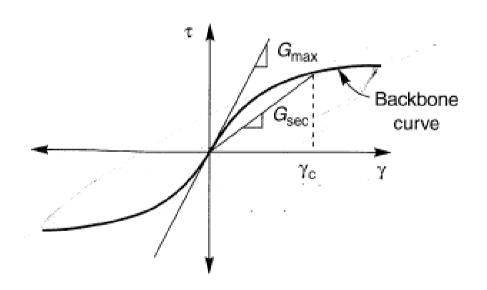


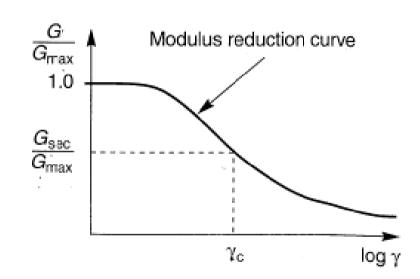




MODELING SOIL RESPONSE UNDER CYCLIC LOADING

Non-linear response ⇒ approximated as linear-equivalent model





Shear stress – strain curve $\tau = \tau(\gamma)$

Shear modulus degradation curve $G = G(\gamma)$







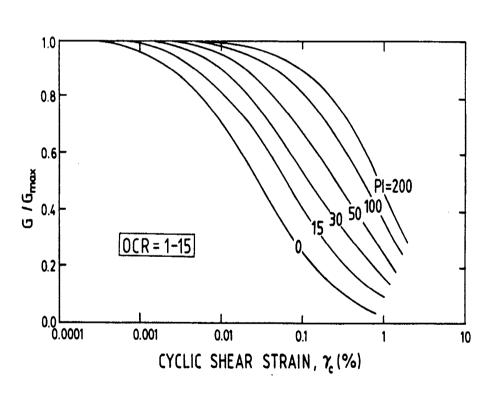


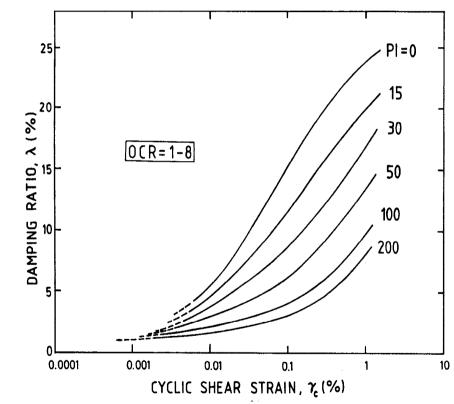




MODELING SOIL RESPONSE UNDER CYCLIC LOADING

Non-linear response ⇒ approximated as linear-equivalent model





Shear stiffness degradation curve $G = G(\gamma)$ Damping ratio degradation curve $D = D(\gamma)$









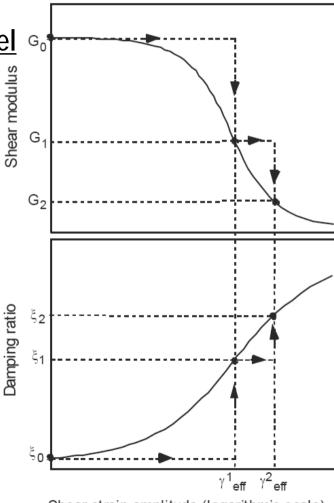




LINEAR-EQUIVALENT VISCOELASTIC CONSTITUTIVE MODEL

Iterative procedure for the linear equivalent model Go

- **1.** Definition for each soil layer of $G=G(\gamma)$ and $D=D(\gamma)$ degradation curves and assignment of initial estimates of $G(\gamma)$ and $D(\gamma)$ corresponding to <u>initial values</u> G_0 and D_0 ;
- **2.** Ground motion is computed for selected G and D pair at each layer; in particular <u>strain histories</u> are calculated;
- **3.** From above <u>effective</u> shear strain γ_{eff} is calculated;
- **4.** From above calculated <u>effective</u> shear strain, new pair of $G(\gamma)$ and $\xi(\gamma)$ are selected using the degradation curves;
- **5.** Steps 2-4 are repeated until the maximum difference between computed shear modulus and damping ratio values in two successive iterations are less than ~5%.



Shear strain amplitude (logarithmic scale)







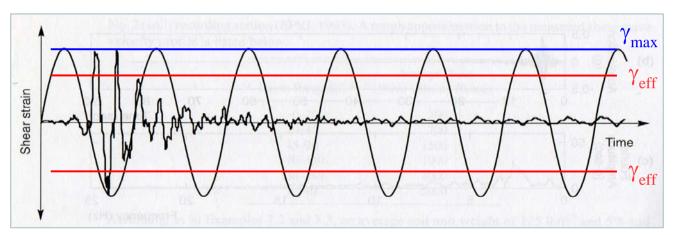






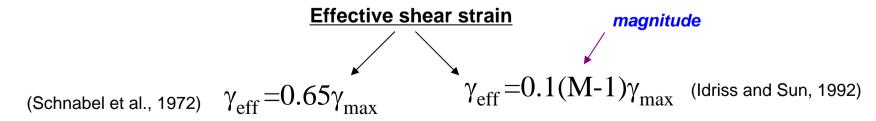
LINEAR-EQUIVALENT VISCOELASTIC CONSTITUTIVE MODEL

Which strain value γ should be used to calculate $G(\gamma)$ and $D(\gamma)$?



Unlike an <u>harmonic</u> wave, earthquake-induced shear strain history in a soil layer is <u>transient</u> and peak strain values do not occur often ⇒ effective strain.

(modified after Kramer, 1996)











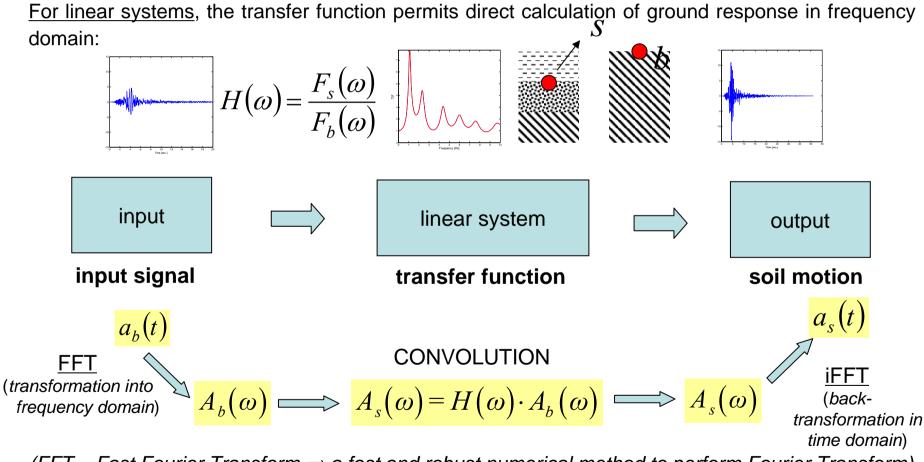




LINEAR-EQUIVALENT VISCOELASTIC CONSTITUTIVE MODEL

Frequency domain analysis

For linear systems, the transfer function permits direct calculation of ground response in frequency



 $(FFT = Fast\ Fourier\ Transform \Rightarrow a\ fast\ and\ robust\ numerical\ method\ to\ perform\ Fourier\ Transform)$













- COMPUTER PROGRAMS FOR GROUND RESPONSE ANALYSIS
 - SHAKE/SHAKE91 (1D,1D), linear-equivalent
 - EERA (1D, 1D), linear-equivalent
 - ONDA (1D, 1D) non-linear
 - CHARSOIL (1D, 1D), non-linear
 - NERA (1D, 1D), non-linear
 - QUAD-4M (2D, 1D), linear-equivalent
 - DESRA (1D, 1D), coupled
 - CYCLID 1D (1D, 2D) coupled
 - DYNA1D (1D, 2D) coupled
 - CYBERQUAKE (1D, 2D) coupled
 - SUMDES (2D, 2D) coupled
 - GEFDYN (3D, 3D), non-linear, coupled
 - DYNAFLOW (3D, 3D) non-linear, coupled
 - FLAC (3D, 3D), non-linear, coupled













LINEAR-EQUIVALENT VISCOELASTIC CONSTITUTIVE MODEL

WEB SITE TO DOWNLOAD EERA:

http://gees.usc.edu/GEES/Software/EERA2000/Default.htm



EERA

Equivalent-linear Earthquake site Response Analysis

Version 2000

This page was last updated on July 02, 2004

EERA is a modern implementation of the equivalent-linear concept of earthquake site response analysis, previously implemented in the original and later versions of SHAKE.

- · System requirement, downloading files and user's manual
- Installing EERA
- Removing EERA
- Automatizing EERA using Visual Basic macros
- · Frequently asked questions
- Reporting problems and asking questions























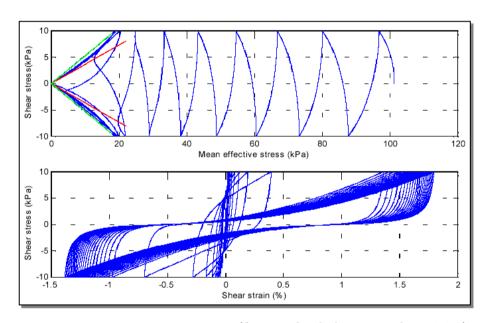




NON-LINEAR CONSTITUTIVE MODEL

Constitutive modeling of soils under earthquake loading:

- linear models (viscoelastic)
- linear-equivalent models
- cyclic non-linear models
- advanced non-linear models



(from Arduino et al., 2002)











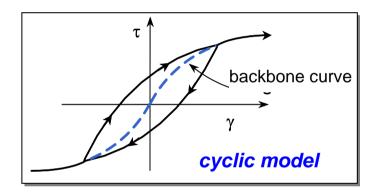


NON-LINEAR CONSTITUTIVE MODEL

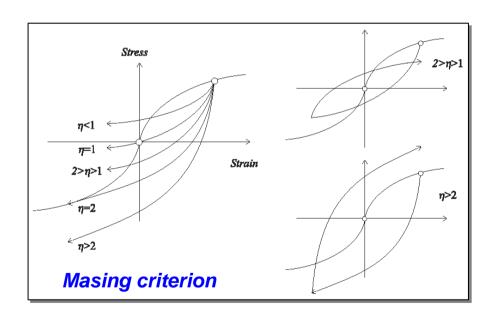
Non-linear cyclic models

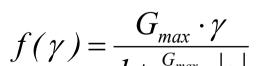


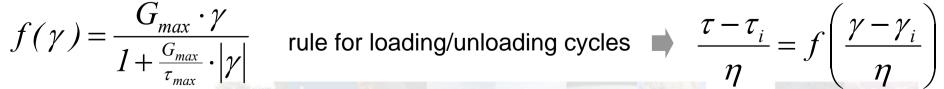
uni-axial stress-path



backbone curve (first loading)



















NON-LINEAR CONSTITUTIVE MODEL

Non-linear cyclic models



uni-axial stress-path

A 1D non-linear cyclic model requires the definition of a backbone curve + unloading-reloading rules. A popular model in geotechnical earthquake engineering for the backbone curve is the Ramberg-Osgood (1943) curve:

Monotonic model: $\frac{\gamma}{\gamma_{y}} = \frac{\tau}{\tau_{y}} + \alpha \frac{\gamma}{|\gamma|} \left| \frac{\tau}{\tau_{y}} \right|^{r}$

 γ : shear strain τ : shear stress γ_y : yield strain τ_y : yield stress

 α : model parameter r: stress exponential γ_0 : strain at reversal t_0 : stress at reversal p: confining stress K: bulk modulus ε_v : volumetric strain

Cyclic model: $\frac{\gamma - \gamma_0}{2\gamma_y} = \frac{\tau - \tau_0}{2\tau_y} + \alpha \frac{\gamma}{|\gamma|} \left| \frac{\tau - \tau_0}{2\tau_y} \right|^r$

where the first reversal is $\gamma\dot{\gamma} < 0$ detected from:

subsequent reversals are $(\gamma - \gamma_0)\dot{\gamma} < 0$ detected from:

Ramberg-Osgood model is originally a 1-D model, however it can be extended to 2D and 3D by assuming that all the deviatoric stress and strain components are linked together independently and volumetric deformation is always elastic $\Rightarrow p = -K\varepsilon_V$











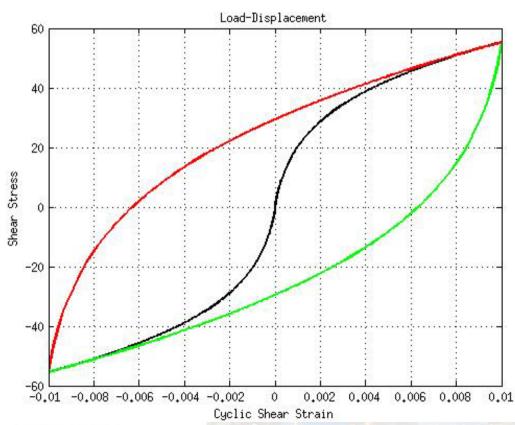
NON-LINEAR CONSTITUTIVE MODEL

Non-linear cyclic models



uni-axial stress-path

Masing's rule (Masing, 1924)



Green line ⇒ **Unloading**

Red line ⇒ Re-loading

Black line ⇒ Backbone curve

It can be observed that green line (unloading) is exactly doubled and reversed version of the backbone curve in positive stress-strain plane.

It can be observed that red line (reloading) is exactly doubled and reversed version of the backbone curve on negative stress-strain plane.











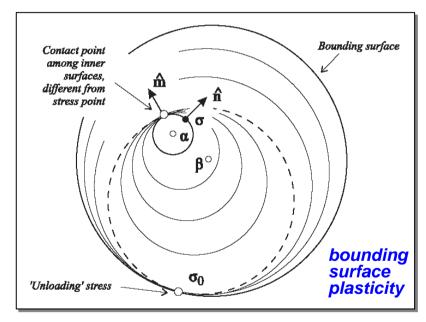


NON-LINEAR CONSTITUTIVE MODEL

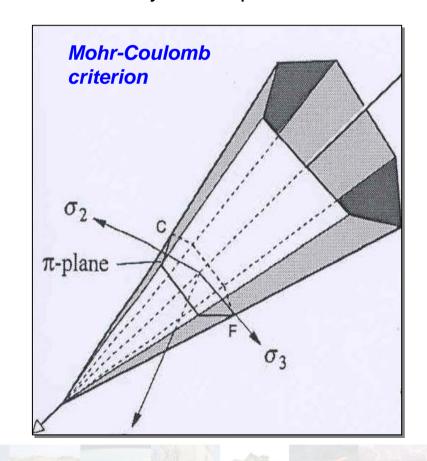
Advanced non-linear models



✓ arbitrary stress-path



- yield surfaces (multiple)
- plastic potential (flow rule)
- hardening rule (isotropic/kinematic)













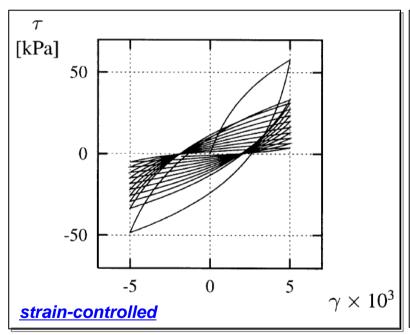


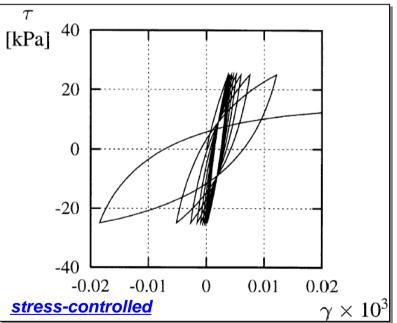
NON-LINEAR CONSTITUTIVE MODEL

Advanced non-linear models



✓ arbitrary stress-path





Undrained cyclic torsional shear simulation (from Osinov, 2003)











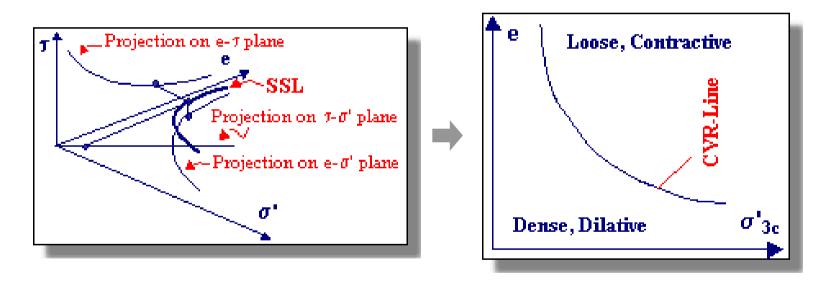


NON-LINEAR CONSTITUTIVE MODEL

Advanced non-linear models



✓ steady-state of deformation



Critical state line in $\{\tau\text{-e-}\sigma'\}$ space (from *Kramer, 1996*)













NON-LINEAR CONSTITUTIVE MODEL

Although equivalent linear models provide reasonable results in many practical problems, it only captures soil response in an approximate manner.

Differently from linear and equivalent linear methods, true non-linear ground response analysis can only be carried out numerically integrating the equations of motion in the <u>TIME DOMAIN</u> ⇒ <u>explicit and implicit finite difference methods</u>

$$\frac{\partial \tau}{\partial z} = \rho \frac{\partial^2 u}{\partial t^2} = \rho \frac{\partial \dot{u}}{\partial t}$$

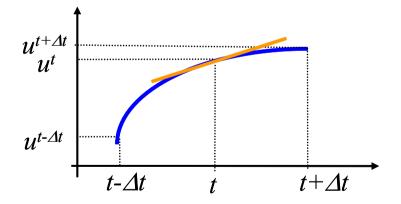
Equation of motion for vertical 1-D propagation of SH waves

Forward difference approximation for u'(t)

$$\frac{\partial u^t}{\partial t} = \frac{u^{t+\Delta t} - u^t}{\Delta t}$$

Forward difference approximation for
$$u''(t)$$

$$\frac{\partial^2 u^t}{\partial t^2} = \frac{u^{t+\Delta t} - 2u^t + u^{t-\Delta t}}{\Delta t^2}$$



Stresses should be obtained from non-linear constitutive law at each time step.













NON-LINEAR CONSTITUTIVE MODEL

STABILITY CONDITION
$$\Delta t \leq \frac{\Delta x}{\beta_i}$$
 Courant-Friederichs-Levy condition

The meaning of Courant-Friederichs-Levy stability condition is that the time step cannot be larger than the time required for any perturbation to propagate over the distance Δx .

If <u>Courant-Friederichs-Levy stability condition</u> is satisfied the error magnitude is bounded and the algorithm is stable.

$$\frac{\text{GRID DISPERSION}}{10} \qquad \Delta x \le \frac{\lambda_{min}}{10} = \frac{\beta_{min}}{10 \cdot f_{max}}$$

For <u>finite difference scheme</u> to be accurate up to a frequency f_{max} , and if the minimum velocity of the model is β_{min} . At least 10 points per minimum wavelength are needed in the finite difference scheme to avoid grid dispersion.





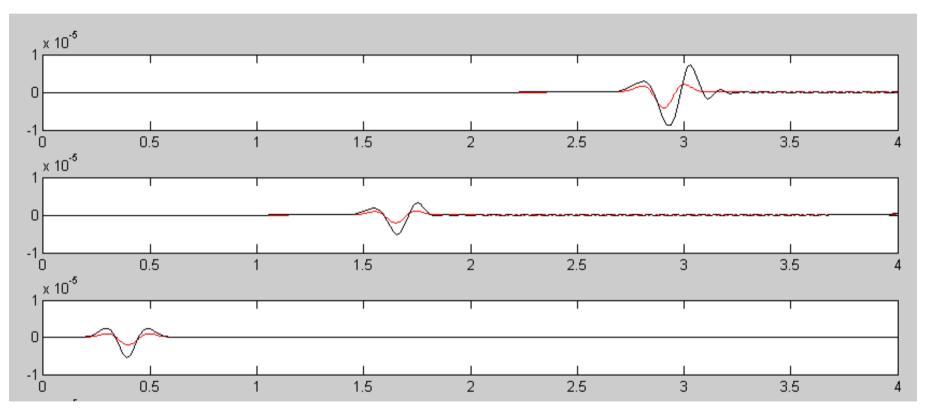








NON-LINEAR CONSTITUTIVE MODEL



red line: signal propagating without dispersion ($\lambda/\Delta x = 10$);

(from Paolucci et al., 2008)

black line: dispersive propagation ($\lambda/\Delta x$ =4). The harmonic components of the signal travel with different phase velocities and the error, initially negligible, grows.





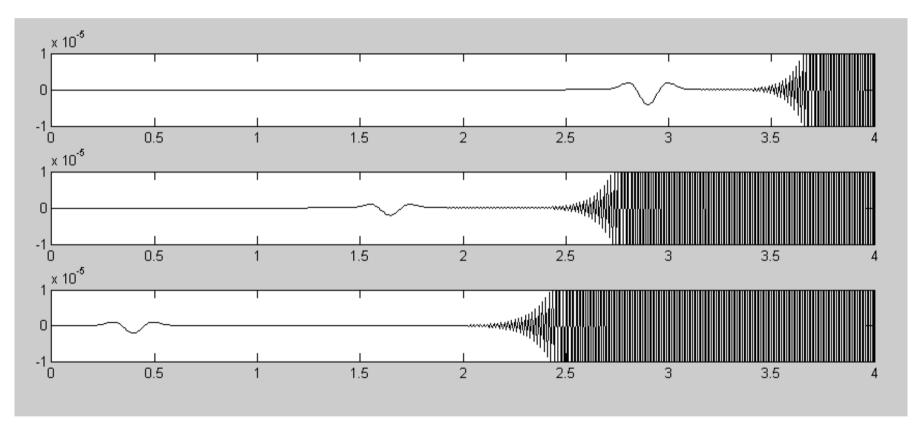








NON-LINEAR CONSTITUTIVE MODEL



(from Paolucci et al., 2008)

The error, initially negligible, grows exponentially all of a sudden.













COMPARISON BETWEEN LINEAR-EQUIVALENT AND NON-LINEAR GRA

EQUIVALENT LINEAR

- Unrealistic resonance may develop Since equivalent linear method uses single elastic modulus and damping ratio value throughout the whole response history, in particular cases where the dominant frequency content in ground motion matches with the strain compatible fundamental frequency of soil deposit, full record length resonance may develop.
- Works in total stress domain Since it works in total stress domain (not effective), phenomena of pore water generation and dissipation may not be modeled.
- Applicable on limited range of strains Equivalent linear analysis method looses its accuracy after cyclic shear strains greater than ~1%
- More practical

Since the transfer functions in frequency domain are well-stated, the computation is straightforward and fast. Application of the method needs less amount of soil related parameters (unit weight, initial rigidity, modulus degradation and damping ratio curves)

NON-LINEAR

- Unrealistic resonance can not develop In non-linear analyses, stiffness of soil changes at every time step (as a function of constitutive relation and stress/strain reversal laws), therefore unlike equivalentlinear method, unrealistic resonance can not develop.
- Can work in effective stress domain Finite difference/element formulation may be stated in also effective stress domain which enhances accurate modeling of solid-pore water interaction inside the soil matrix.
- Applicable on whole range of strains Is applicable throughout all strain ranges, without any limitation.
- More demanding

Theoretical solution is not present, therefore numerical timestepping is needed. For accuracy and stability, time step is generally small, therefore analyses take much longer. In addition to eq-linear parameters, needs extra soil-related parameters (strain-stess reversals, constitutive law, etc.)













COMPARISON BETWEEN LINEAR-EQUIVALENT AND NON-LINEAR GRA

EQUIVALENT-LINEAR

- Can not model yielding (failure) By definition, soil is modeled as an elastic material, therefore soil failure can not be captured.

- Can not model permanent displacements Since the soil model is elastic, after the transient motion (i.e. input round motion) finishes, soil deposit returns to its original orientation.

NON-LINEAR INELASTIC

- Can model yielding (failure) Even the most fundamental inelasticity law (i.e. elastic-perfectly plastic Mohr-Coulomb) can capture soil yielding by using single yielding surface. More advanced models (models having a decent yield, flow and hardening rules) are capable of modeling soil yielding more accurately by using multi-yield surfaces.
- Applicable on whole range of strains Sometimes, permanent displacement can be an important parameter defining the performance of a geotechnical system (for seismic analysis of dams/embankments/slopes). Since, inelastic models can define yielding, as a consequence irreversible deformations also develops in the soil deposit.













Stochastic ground response analyses













In 2004 David Boore wrote a paper on the JEE with a rather provocative title: "Can Site Response Be Predicted?"

Journal of Earthquake Engineering, Vol. 8, Special Issue 1 (2004) 1–41 © Imperial College Press



CAN SITE RESPONSE BE PREDICTED?

DAVID M. BOORE

US Geological Survey, 345 Middlefield Road, MS 977, Menlo Park, CA 94025, USA

Citation:

"Reliable quantitative predictions of site response are needed for engineering design — thus the question posed in the title: "Can site response be predicted?". I think that many in the field would answer "yes", but I think that the answer to the title question is: "it depends". It depends on what kind of site response is being predicted and what accuracy is needed in the prediction." (David M. Boore, 2004)





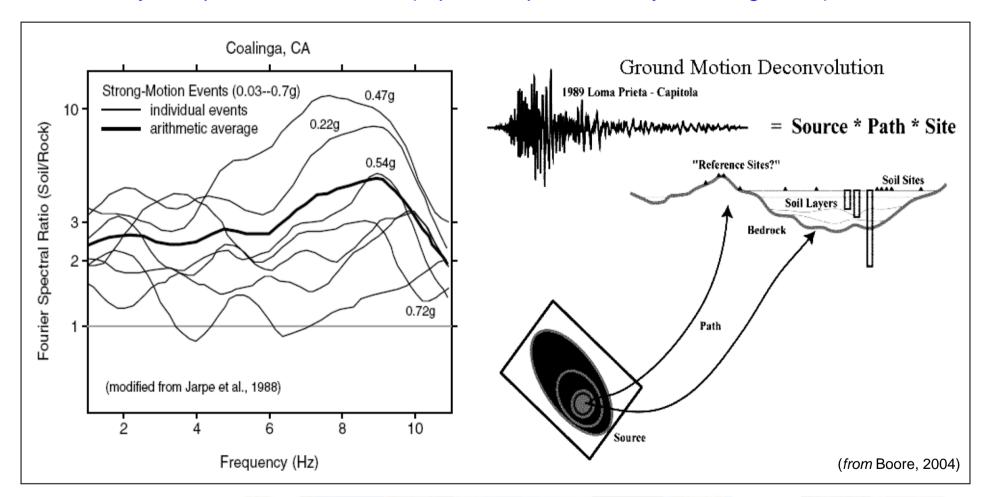








<u>Variability of Input Ground Motion</u> (eqke-to-eqke variability at a single site):









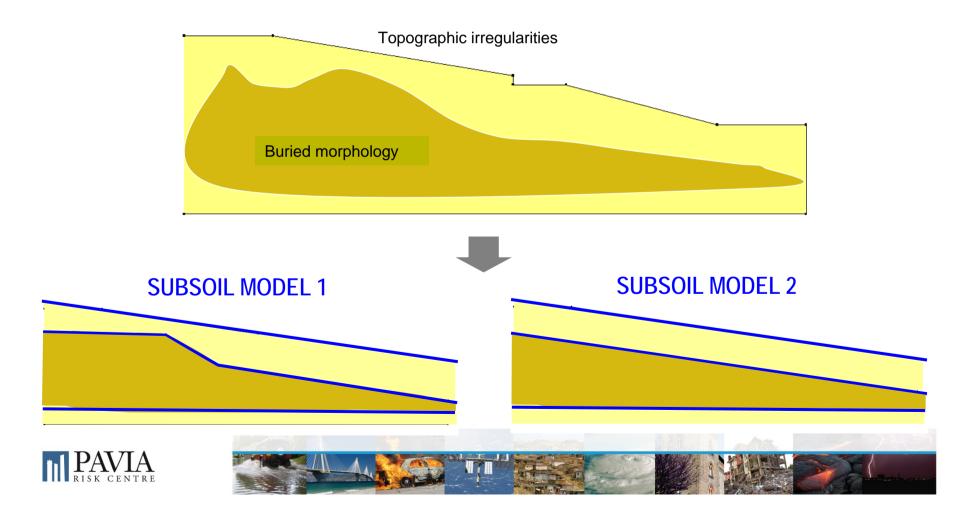






Variability of Geotechnical Modelling:

REAL SUBSOIL CONDITIONS AT A GIVEN SITE



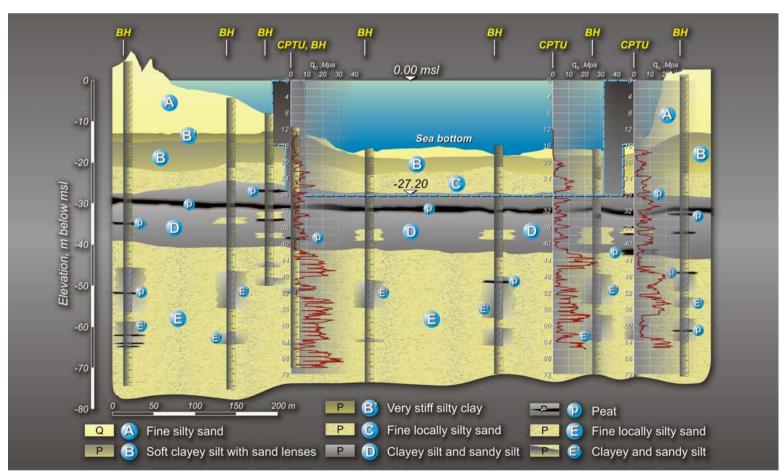








Variability of Geotechnical Modelling:



⇒ What geotechnical model?

(from Jamiolkowski et al., 2007)





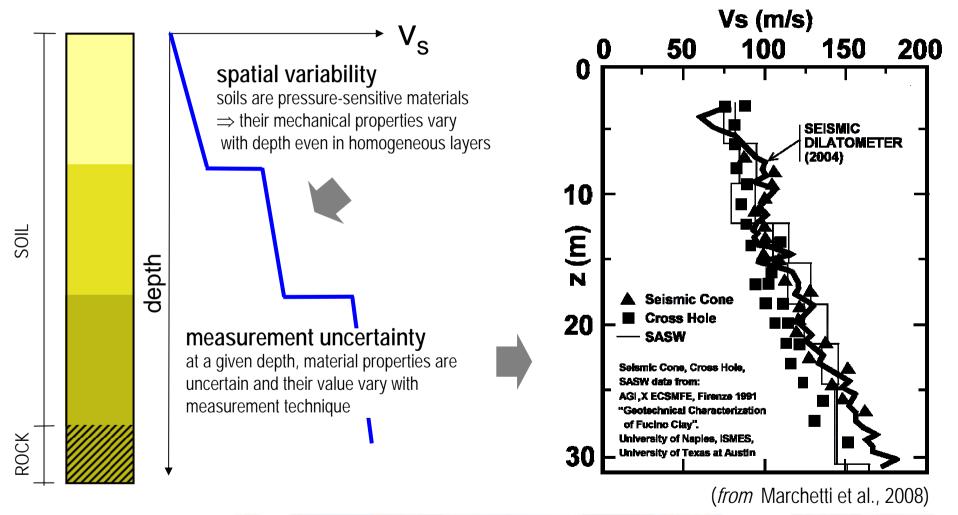








Variability of Geotechnical Properties:















Stochastic ground response analysis

Deterministic (Parametric) over Stochastic Ground Response Analysis:

Deterministic: a deterministic GRA is based on assuming a SINGLE geotechnical model to which is associated a SINGLE set of geotechnical/material parameters. The analysis is then run making reference to a SINGLE seismic excitation.

<u>No consideration</u> is given for several sources of uncertainties that affect the geotechnical model, the material parameters and seismic input thereby neglecting their influence on site response.

Parametric analyses (sensitivity studies) represent an improvement however they fail to fully and systematically address treatment of various sources of uncertainty in a unified framework.

STOCHASTIC SITE RESPONSE ANALYSIS



- Opportunity to assess the sensitivity of the results to the uncertainty of seismic input;
- Opportunity to assess the sensitivity of the results to the uncertainty of model parameters;
- Opportunity to identify which are the parameters whose uncertainty contribute the most to the uncertainty of site response → require definition of response functions
- Opportunity to optimize funds allocation for geotechnical site investigation/characterization





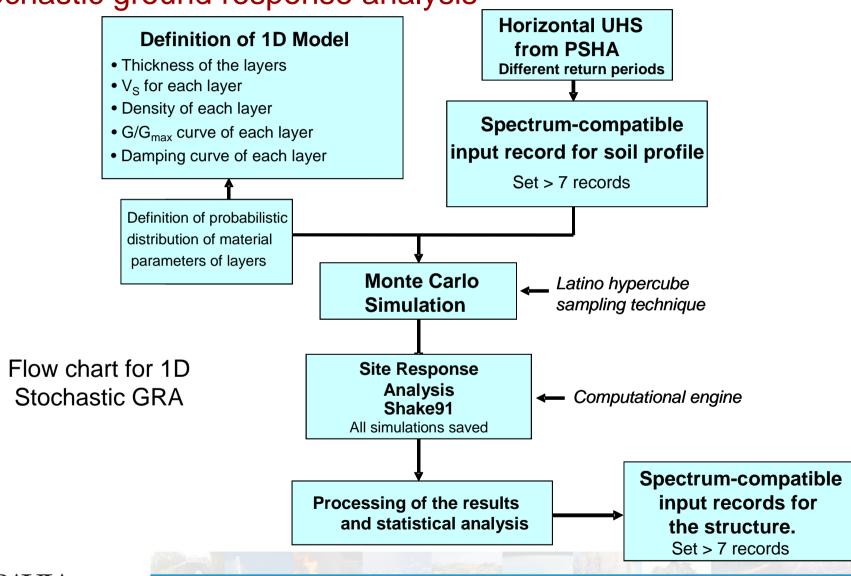








Stochastic ground response analysis







Case study









Cathedral with the world largest elliptical dome in Northern Italy:





"Regina Montis Regalis" Sanctuary is located at Vicoforte (CN), in the Southwest of the Piedmont region in Northern Italy

In 1596 Charles Emmanuel I of Savoy commissioned the construction of a large Sanctuary from the court architec Ascanio Vittozzi.













Cathedral with the world largest elliptical dome in Northern Italy:







S.Pietro

S.Maria del Fiore

Mausoleo Gol Gumbaz

		Locality	Construction Period	Diameter	Proyect
1	Pietro	Rome (Italy)	1546-1593	42.84 m	Michelangelo
2	S.Maria del Fiore	Florence (Italy)	1423-1425	41.7 m	Brunelleschi
3	Mausoleo di Gol Gumbaz	Bijiapur (India)	1636-1660	37.9 m	Yaqut of Dabul
4	Vicoforte di Mondovi	Vicoforte (Italy)	1701-1750	37.15- 24.8 m	Gallo
5	Hagia Sofia	Istambul (Turkey)	532-537	33.23 m	Antemio di Tralles,
					Isidoro di Mileto

Elliptical dome

		Locality	Construction Period	Diameter	Proyect
1	Vicoforte di Mondovi	Vicoforte (Italy)	1701-1750	37.15-24.8 m	Gallo
2	S.Andrea al Quirinale	Rome (Italy)	1658	26-17 m	G.L. Bernini
3	S.Carlos alle Quatro Fontane	Rome (Italy)	1638	25-19 m	F. Borromini
4	Convento Bernardas	Alcalá (Spain)	1626	25-17.5 m	S.Plaza





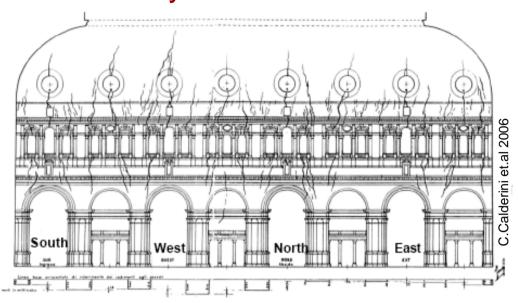








Case study





In 1985, concerns over such severe cracking, prompted the decision to undertake monitoring and strengthening works.

In recent years a new project was started for a thorough renovation of the monitoring system

Procedure already started for the inclusion of Vicoforte Basilica in the UNESCO world heritage list





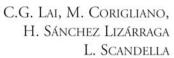












Motivation of study:

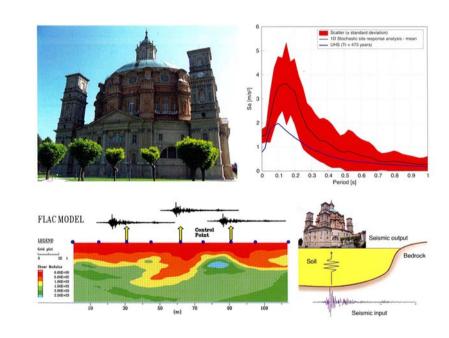
Case study

Study was performed in the framework of a more wide-ranging research aimed at **defining the seismic input** for dynamic analyses of the Basilica.

Work carried out by EUCENTRE within research contract undersigned with the Administration of Sanctuary for the monitoring and survey of the "Regina Montis Regalis Basilica".

Research was supported by *Fondazione Cassa di Risparmio di Cuneo*.

Definition of Seismic Input at the "Regina Montis Regalis" Basilica of Vicoforte, Northern Italy





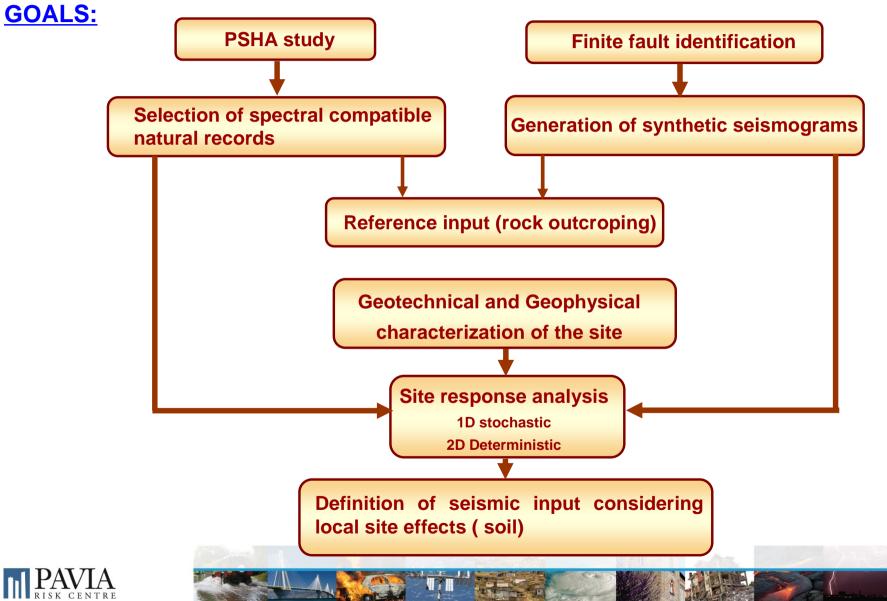












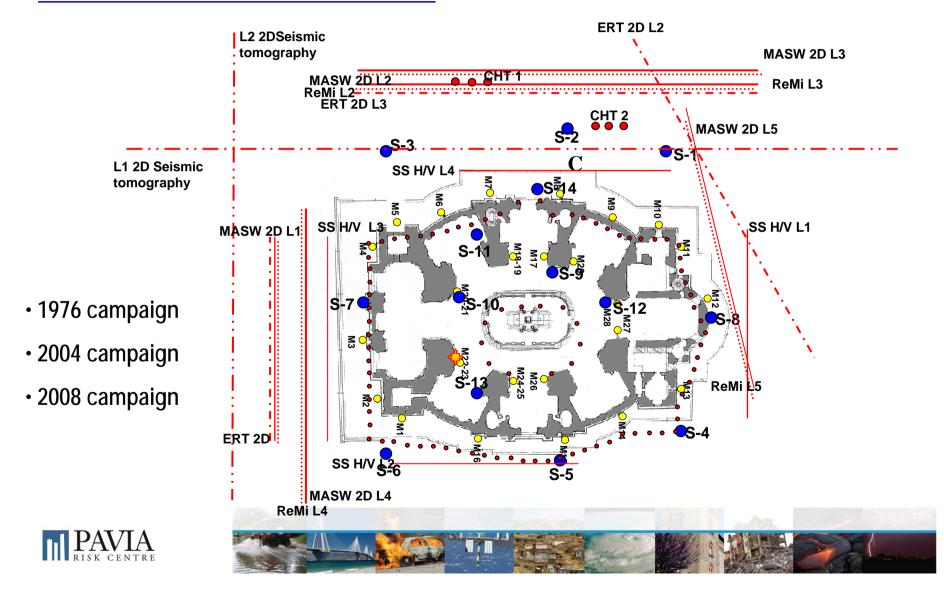








Geotechnical site characterization:



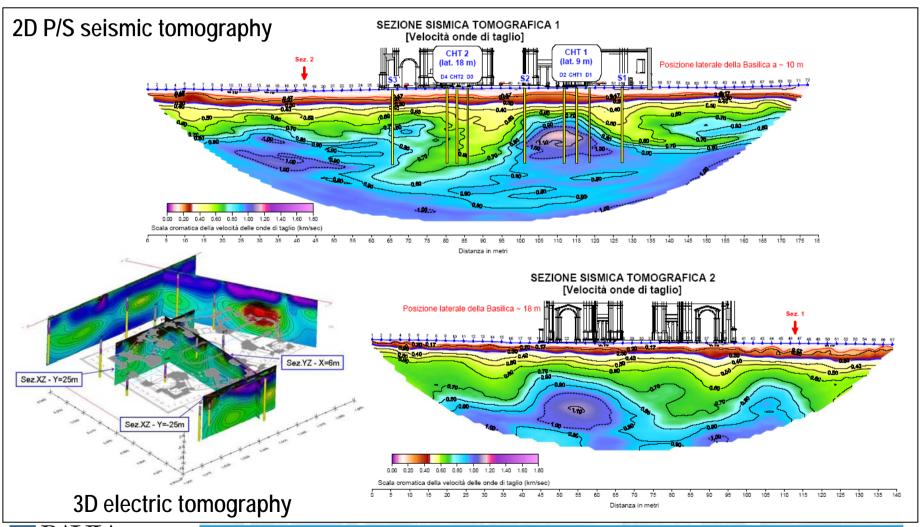








Geotechnical site characterization:







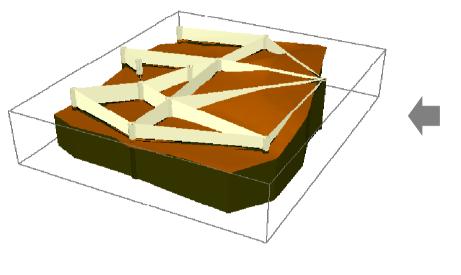






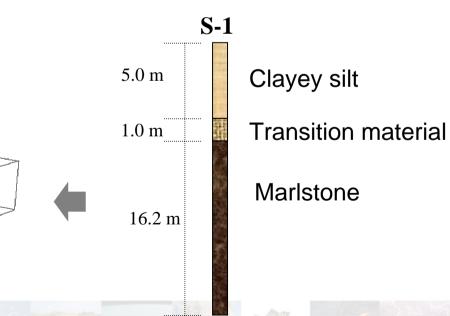


Geotechnical site modelling:



Lithostratigraphic reconstruction of soil deposit below the cathedral.

A 3D subsoil model was obtained by interpolating the lithological data from borehole and geophysical data.





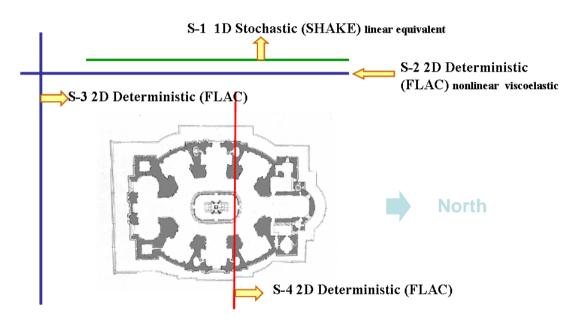






Stochastic site response analysis:

Given the characteristics of subsoil at the site, 4 different sections were chosen to carry out GRA:



Section	Direction	Test used to generate section	Type of Analysis	Software used
S-1	NS-outside the Basilica	Boreholes/Cross hole/ MASW	1D Stochastic	SHAKE
S-2	NS-outside the Basilica	2D Seismic Tomography	2D Deterministic	FLAC
S-3	EW-outside the Basilica	2D Seismic Tomography	2D Deterministic	FLAC
S-4	EW-below the Basilica	Boreholes/ Geostatistics	2D Deterministic	FLAC







Stochastic site response analysis:

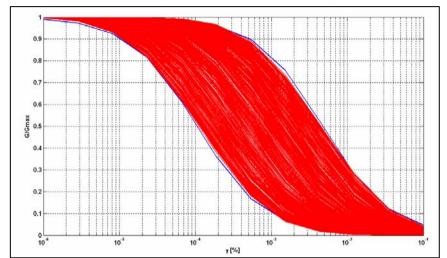
- Seismic excitation
- Thickness of individual layers.
- V_S for each layer.
- Density of each material
- G/G_{max}/Damping degradation curves

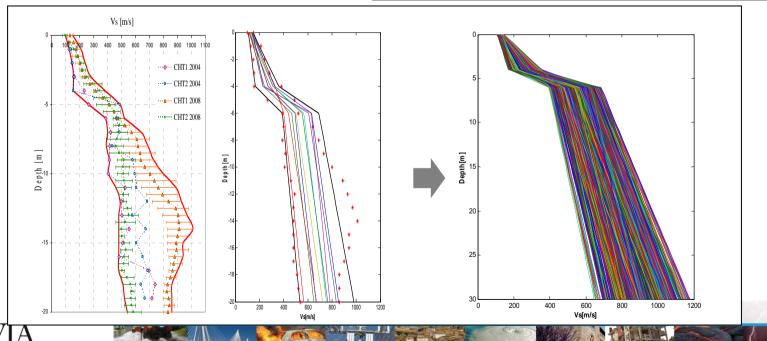












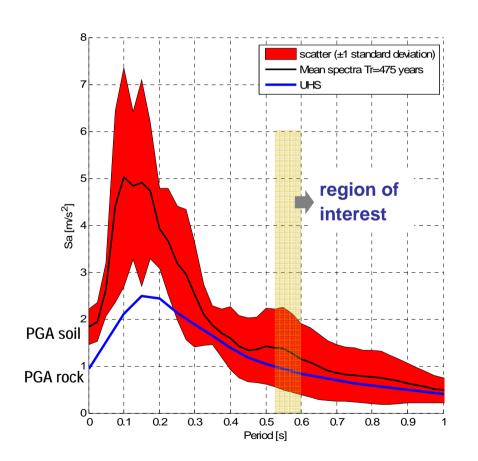






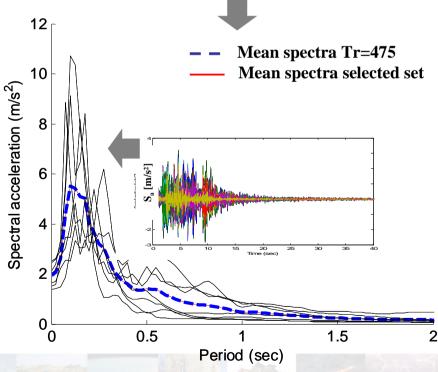


Stochastic site response analysis:



Mode of vibration	Frequency (Hz)
1	1.67
2	1.77
3	1.78

Selection of time histories from stochastic site response analysis















Remarks

- <u>Large variability</u> of site response is observed at a given site due to different seismic inputs and for a given input (predictions) due to <u>uncertainty</u> in subsoil modelling and geotechnical parameters.
- Parametric (i.e. deterministic) site response analyses are inadequate to handle this problem. Moreover <u>critical combinations of geotechnical parameters</u> and seismic input that may induce large ground amplification are completely overlooked by such analyses.
- Stochastic site response analysis allow to assess sensitivity of results to uncertainty of model parameters and of reference seismic input. This may be used to optimize resources and funds in geotechnical site investigation and characterization.
- Methodology was set-up to perform 1D linear-equivalent, fully stochastic site response analyses taking into account uncertainty of seismic input & model parameters.
 Procedure allows selection of spectrum-compatible records with reference to mean spectrum.













Model parameters for ground response analyses













SOME DEFINITIONS

<u>Linear cyclic threshold shear strain</u>: Shear strain threshold until which the theory of viscoelasticity is valid. Reference value of $\gamma_{tl} \sim \gamma_{tv}/30$ (Vucetic, 1994).

As PI=LL-PL increases γ_{tl} increases.

Backbone (skeleton) curve: The locus of points corresponding to the tips of hysteresis loops of various strain amplitudes. Its slope at origin is G_{max} . For cyclic strains greater than linear cyclic threshold shear strain $G(\gamma)/G_{max}<1$.

Modulus reduction (degradation) curve (G(\gamma)/G_{max}): The variation of modulus ratio with increasing shear strain. Defines the non-linearity of the soil medium.

Initial (Elastic) shear modulus: Shear modulus that is valid until cyclic threshold shear strain. This value is a very useful quantity also to define soil characterization.













SOME DEFINITIONS

<u>Volumetric threshold shear strain</u>: Shear strain threshold corresponding to initiation of gross sliding which results in permanent particle re-orientation (i.e. volume change: dilation/contraction) when the soil element is sheared.

From particulate theory, the volumetric threshold shear strain for monogranular soil matrix may be stated as (Kramer, 1996)

$$\gamma_{n} \cong 2.08 \frac{(2-v)(1+v)f}{(1-v^2)^{1/2}E^{2/3}} (\sigma^1)^{2/3} \qquad \text{or} \qquad \text{for 25 kPa} < \sigma^2 < 200 \text{ kPa range } \gamma_{n} (\%) = 0.000175 (\sigma^1)^{2/3} (\sigma^2 \text{ in psi})$$

For Quartz solid particles -> E=7.6e7 kPa (1.1e7 psi), v=0.31, f=0.50

f: coefficient of friction of soild particles (in microscale, not of soil matrix in macroscale)

v: Poisson's ratio for solid particles (in microscale, not of soil matrix in macroscale)

E: Elastic Modulus for solid particles (again in microscale)

As PI=LL-PL

increases γ_{ty} increases.











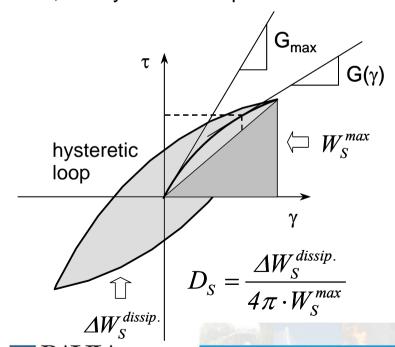


EQUIVALENT-LINEAR MODELS

If these conditions are satisfied:

- free-field ground
- soil element located at large depth
- soil element is subjected to perfectly symmetric cyclic loading

Then, the hysteresis loop of the soil at that point becomes to be:



Equivalent linear theory defines two important strain dependent values:

- 1. Secant shear modulus
- 2. Damping ratio of each cycle

Then use theory of linear viscoelasticity









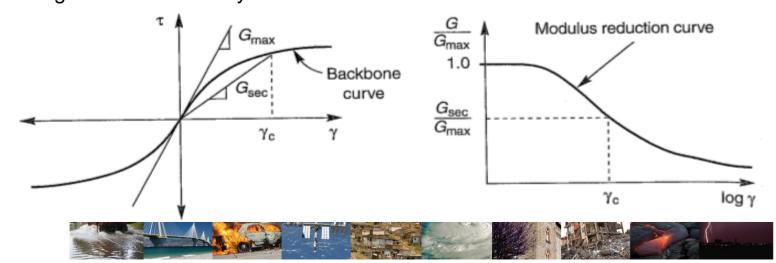
EQUIVALENT-LINEAR MODELS

1. Secant shear modulus:

Is a function of cyclic shear strain amplitude, void ratio, mean effective confining stress, plasticity index, overconsolidation ratio, number of loading cycles, etc...

At low strains, secant shear modulus is high (and for the strains below linear cyclic shear threshold, it is Gmax), as cyclic shear strain increases secant shear modulus decreases (effect of non-linearity)

The locus points corresponding to tips of the hysteresis loops of various cyclic strain amplitudes represents the <u>backbone curve</u> (it is like the pushover curve in structures). If all the secant moduli on this graph are scaled by maximum shear modulus (Gmax), then modulus degradation curve may be obtained.













EQUIVALENT-LINEAR MODELS

1. Secant shear modulus:

Therefore, secant shear modulus is represented by the pair of parameters:

- a. Initial (elastic) shear modulus (Gmax)
- b. Shear modulus reduction curve (G/Gmax)

cross-hole, down-hole

a. Initial (elastic) shear modulus (Gmax)



In situ tests: $G_{max} = \rho V_s^2$ or SPT, CPT tests

In absence of in-situ data, several correlations may also be used:

$$G_{\text{max}} = 1000 \text{ K}_{2.\text{max}} (\sigma'_{\text{m}})^{0.5}$$

For soil
$$\rightarrow$$
 G_{max}=625 F(e) (OCR)^k p_a¹⁻ⁿ (σ'_m)ⁿ \longleftarrow Use consistent stress units!

For specific soil \rightarrow e.g. Fioravante 2000 for Ticino sand: G_{max} =60000 $e^{-0.8}$ $(\sigma'_v/p_a)^{0.272}$ $(\sigma'_h/p_a)^{0.168}$













EQUIVALENT-LINEAR MODELS

1. Secant shear modulus:

b. Shear modulus degradation curves (G/Gmax)

<u>In the early years</u> → generations of <u>discrete</u> modulus degradation curves

For sand: Seed and Idriss (1970), Iwasaki et al (1978), Sun et al (1988)

For clays: Vucetic and Dobry (1991)

For gravel: Seed et al (1986), Yasuda and Matsumoto (1993)

For rock: Schnabel et al. (1972)

<u>In recent years</u> → generations of <u>continuous</u> modulus degradation curves as a function of void ratio, mean effective confining stress, OCR, PI, etc.

e.g. Ishibashi and Zhang (1993), Darendeli (2001)

Darendeli (2001) model is useful because is developed over a broad dataset.











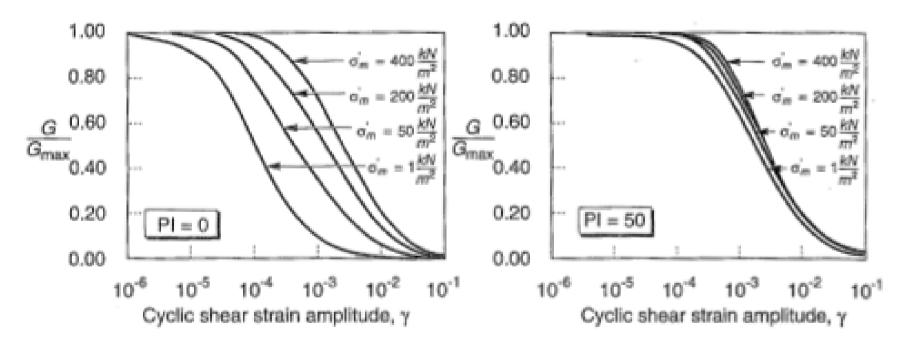


EQUIVALENT-LINEAR MODELS

1. Secant shear modulus:

b. Shear modulus degradation curves (G/Gmax)

Ishibashi & Zhang (1993)















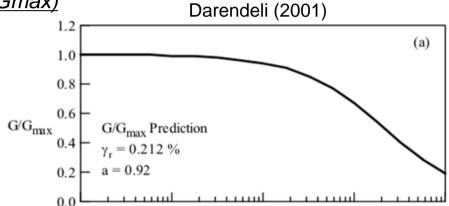
EQUIVALENT-LINEAR MODELS

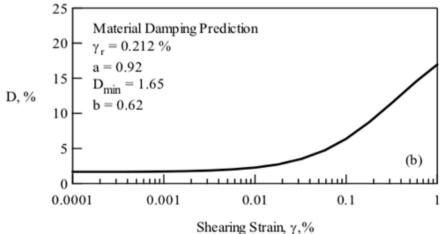
1. Secant shear modulus:

b. Shear modulus degradation curves (G/Gmax)

$$\frac{G}{G_{\text{max}}} = \frac{1}{1 + \left(\frac{\gamma}{\gamma_r}\right)^a}$$

$$\begin{split} \frac{G}{G_{\max}} &= \frac{1}{1 + \left(\frac{\gamma}{\gamma_r}\right)^a} \\ D_{Adjusted} &= b * \left(\frac{G}{G_{\max}}\right)^{0.1} * D_{Ma \sin g} + D_{\min} \end{split}$$













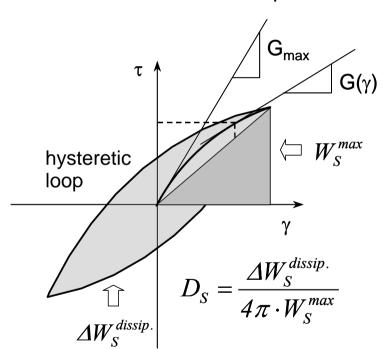




EQUIVALENT-LINEAR MODELS

2. Damping ratio:

Represents the energy dissipated during a hysteretic cycle corresponding to any cyclic shear strain value. It is computed from laboratory data.



Until the shear strain does not exceed the cyclic linear threshold shear limit, soil exhibits viscoelastic behaviour and this is described by D_{min} and G_{max} .

After exceeding this limit γ^t_l , the main cause of damping is hysteretic (due to non-linearity). Damping ratio increases as the magnitude of cyclic shear strain increases.

If the material exhibit more inelastic behaviour it will dissipates more energy. Stiffness and damping degradation curves follow opposite trends.













EQUIVALENT-LINEAR MODELS

What are the factors that affect modulus degradation and damping curves ?

- Cyclic shear strain
- Confining pressure
- Plasticity index
- Void ratio
- OCR
- Number of loading cycles
- Loading frequency
- Cementation
- Geologic age

most dominant factors!

Increasing Factor	G(γ)/Gmax	DR(γ)
Cyclic shear strain	Decreases	Increases
Confining pressure	Increases	Decreases
Plasticity index	Increases	Decreases
Void ratio	Increases	Decreases
OCR	N/S	N/S
Cementation	May increase	May decrease
Geologic age	Increases	Decreases

N/S: not significant







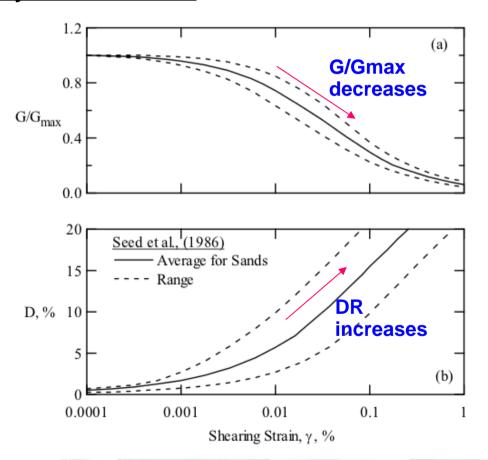






• EQUIVALENT-LINEAR MODELS

Influence of cyclic shear strain:



As cyclic shear strain increases

(from Seed 1986; Darendeli 2001)







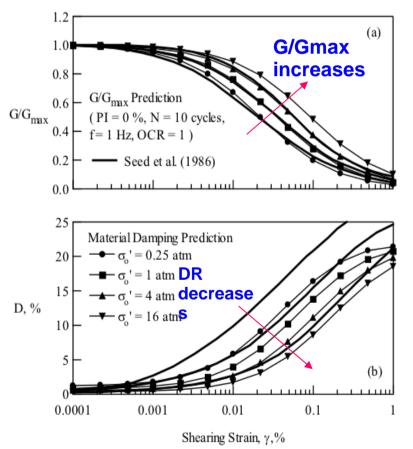






EQUIVALENT-LINEAR MODELS

Influence of confining pressure:



As mean effective confining pressure increases







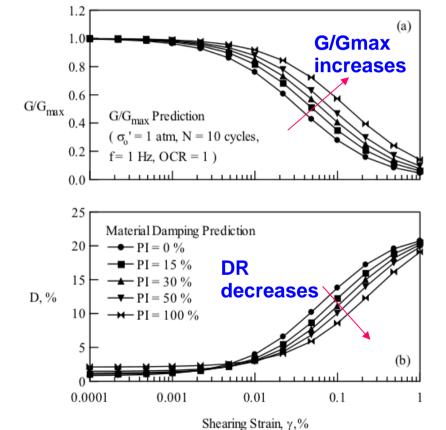






• EQUIVALENT-LINEAR MODELS

Influence of confining pressure:



As PI increases







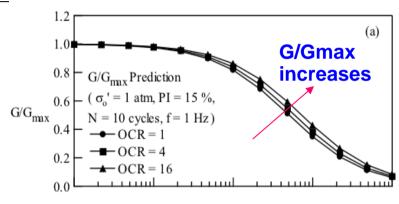






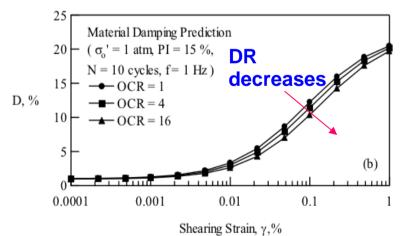
• EQUIVALENT-LINEAR MODELS

Influence of OCR:



Increase is not significant





Decrease is not significant

(from Darendeli 2001)







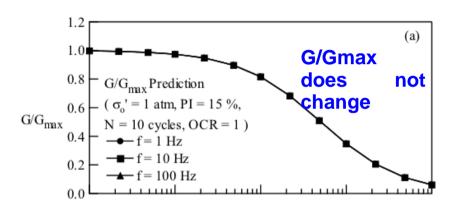


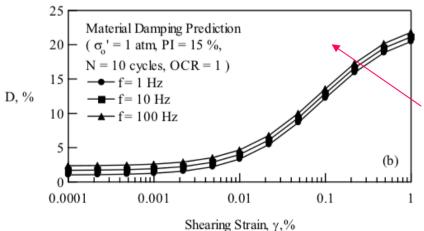




• EQUIVALENT-LINEAR MODELS

Influence of loading frequency:





As freq increases

DR increases, but not very significant

(from Darendeli 2001)







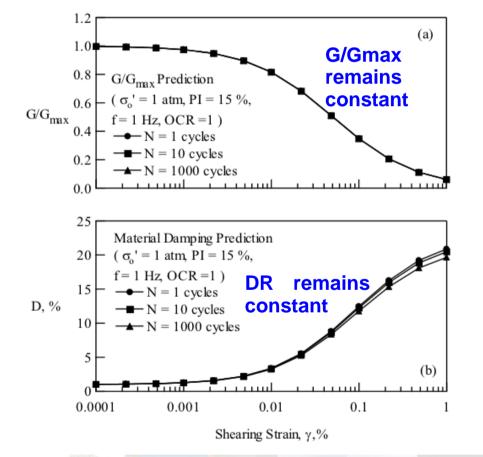






• EQUIVALENT-LINEAR MODELS

Influence of successive cycles:



As N increases

(from Darendeli 2001)













NON-LINEAR MODELS

Stress-strain behaviour may be better modelled by using <u>non-linear models</u>. In such models, it is also possible to introduce soil "strength", which means "inelasticity" is allowed.

To construct a cyclic non-linear material model:

- Backbone curve
- Rules defining "loading" and "reloading" paths

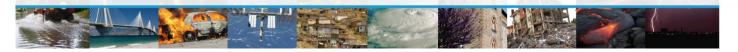
Backbone curves may be defined by:

- Polynomial fitting to an available experimental modulus degradation curve (hyperbolic, etc)

Reloading and unloading paths may be defined by applying either of:

- Coupling predefined backbone curve with unloading and reloading rules such as Masing's rule, extended Masing's rule, Cundall-Pyke, etc.
- Using a cyclic constitutive model that is able to represent the backbone curve and having loading, reloading, and unloading rules defined.







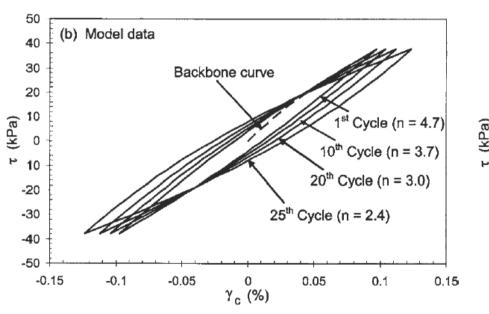


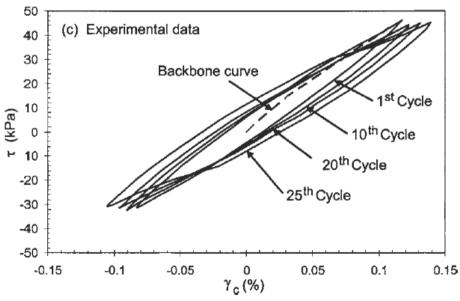




NON-LINEAR MODELS

Cyclic model based on Ramberg-Osgood coupled with modified Masing rule





Comparison between model prediction and experimentally determined stress strain loops

(from Lo Presti et al. 2006)













A brief introduction to 2D/3D ground response analyses













STATEMENT OF THE PROBLEM

<u>Modifications of characteristics of ground motion</u> caused by local geological-geomorphological-geotechnical conditions:

- Lithostratigrafic amplification
- Topographic amplification

local site effects

LITHOSTRATIGRAFIC AMPLIFICATION

1D Ground Response Analysis

<u>Vertical propagation of waves</u> in soil deposits constituted by a stack of plane and parallel layers with contrast of mechanical impedance from bottom to top

2D/3D Ground Response Analysis

Propagation of waves in complex geological configurations with arbitrary orientation of incident waves and generation of diffractive/scattering phenomena







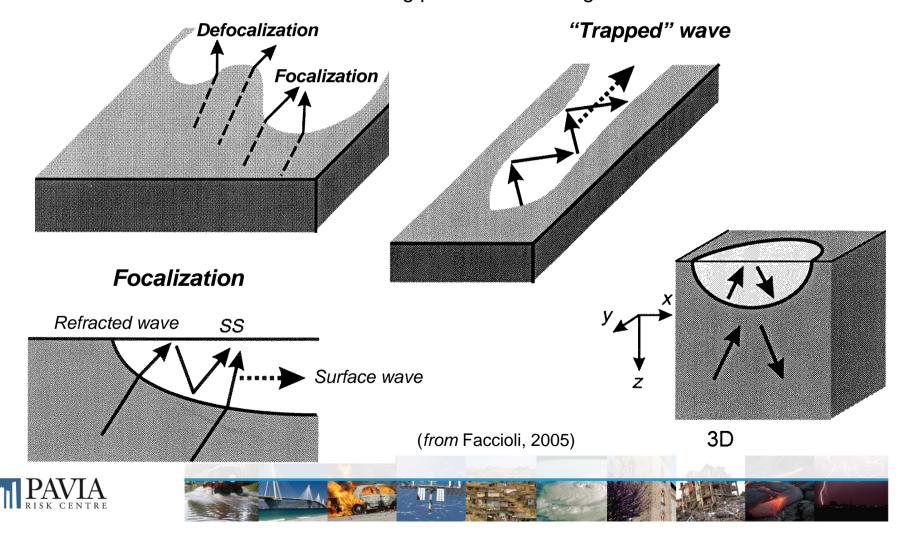






STATEMENT OF THE PROBLEM

Examples of 2D and 3D site effects in a valley or at an alluvial basin. Ground amplification arises as a result of diffraction and scattering phenomena with generation of surface waves



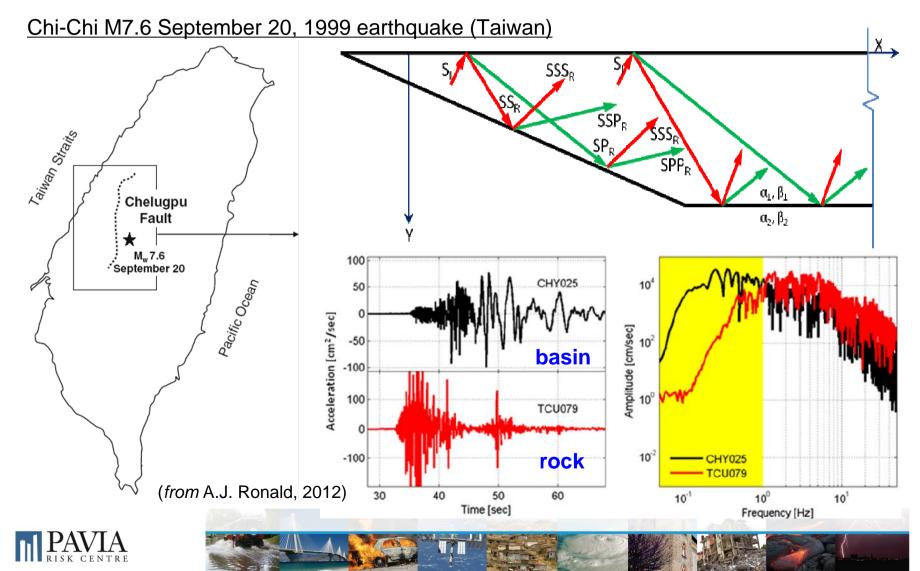








• 2D LITHOSTRATIGRAFIC AMPLIFICATION





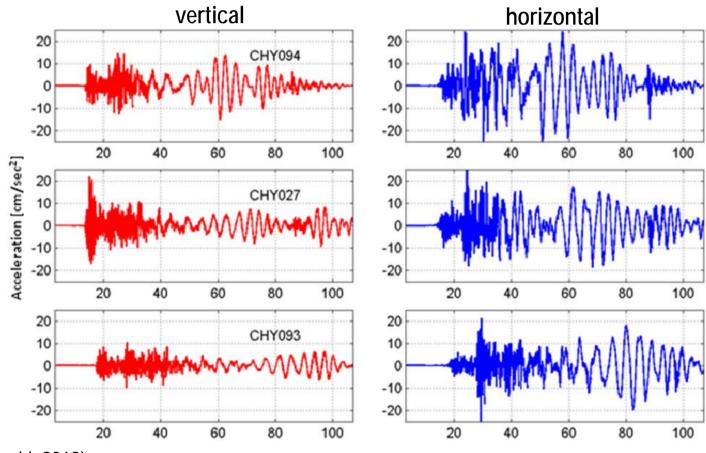






2D LITHOSTRATIGRAFIC AMPLIFICATION

Chi-Chi M7.6 September 20, 1999 earthquake (Taiwan)













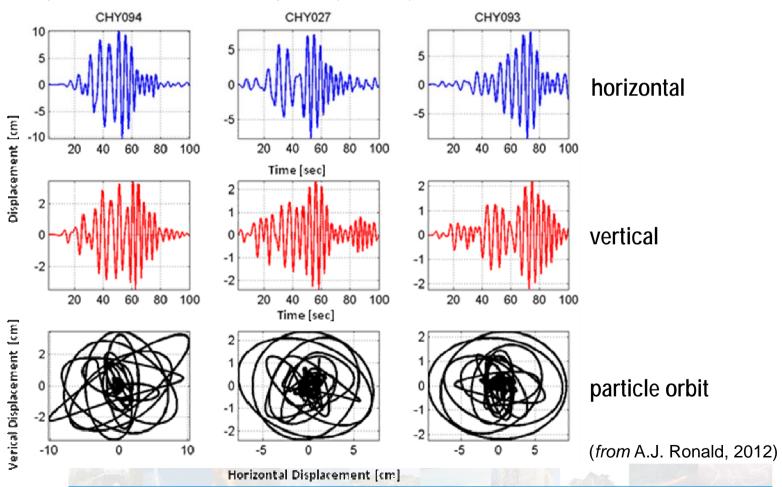






2D LITHOSTRATIGRAFIC AMPLIFICATION

Chi-Chi M7.6 September 20, 1999 earthquake (Taiwan)













• 2D LITHOSTRATIGRAFIC AMPLIFICATION

3D numerical simulation of seismic wave propagation at Grenoble valley (Stupazzini et al., 2009)









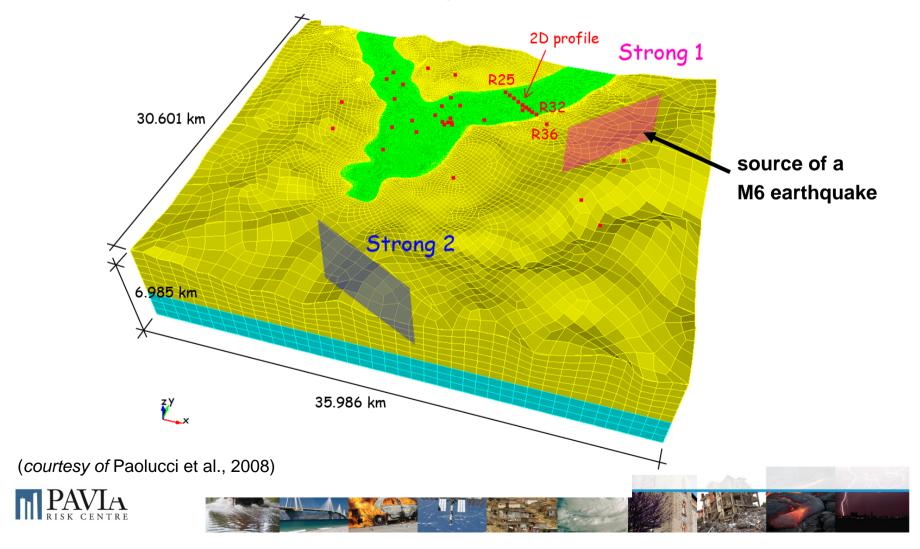






• 2D LITHOSTRATIGRAFIC AMPLIFICATION

3D numerical simulation of seismic wave propagation at Grenoble valley (Stupazzini et al., 2009)





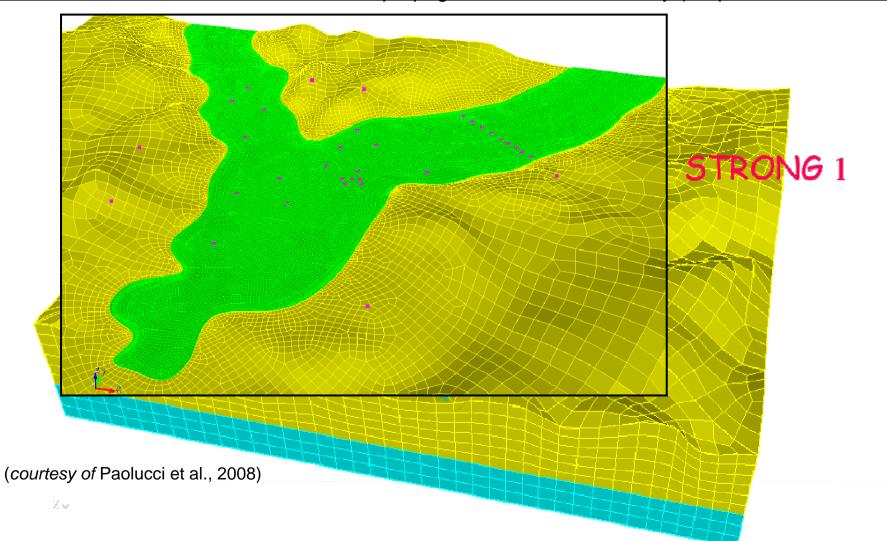






• 2D LITHOSTRATIGRAFIC AMPLIFICATION

3D numerical simulation of seismic wave propagation at Grenoble valley (Stupazzini et al., 2009)







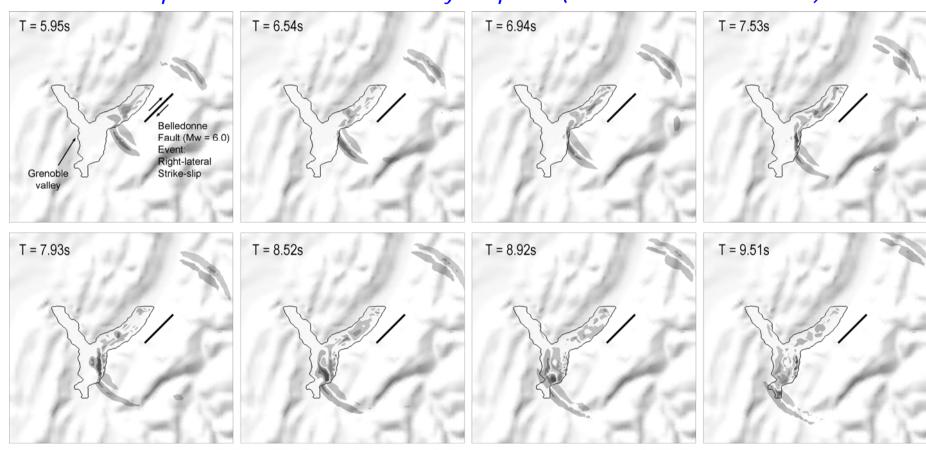




2D LITHOSTRATIGRAFIC AMPLIFICATION

3D numerical simulation of seismic wave propagation at Grenoble valley (Stupazzini et al., 2009)

Snapshots of the Fault Normal Velocity Component (Nucleation at the Fault Centre)



(courtesy of Paolucci et al., 2008)







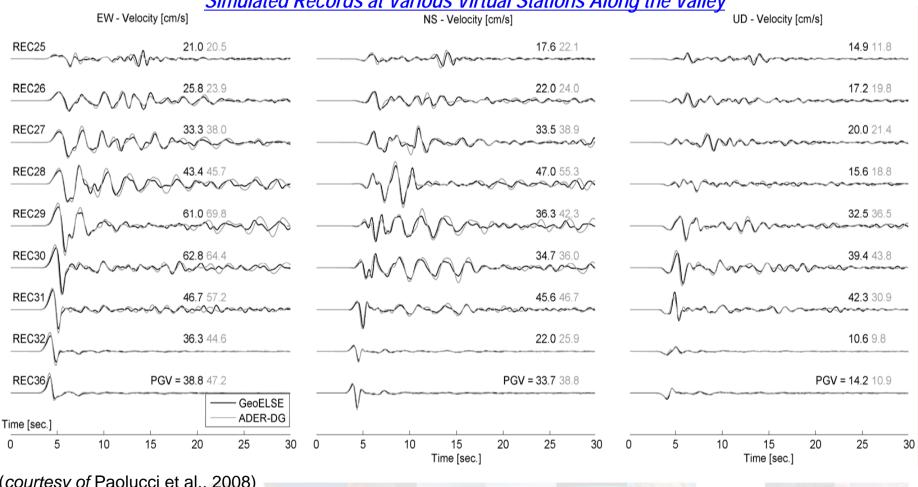






2D LITHOSTRATIGRAFIC AMPLIFICATION

Simulated Records at Various Virtual Stations Along the Valley













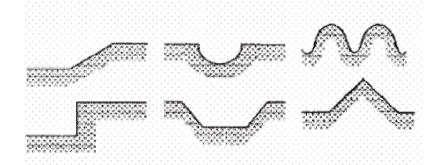




STATEMENT OF THE PROBLEM

TOPOGRAPHIC OR GEOMORPHOLOGICAL AMPLIFICATION

<u>Geometric phenomenon</u> of focalization/de-focalization of the trajectories of propagation of seismic waves in particular types of geomorphological configurations like steep slopes, crests, hills, ridges, trenches, canyons.



slopes trenches

canyon

ridges crests Factors of topographic amplification (S_T)

Morphol	Mean slope	S _T	
Steep isolated slopes			<1.2
Width at the crest much smaller than at the base	a	15° - 30°	<1.2
		> 30°	<1.4

(Eurocode 8-Part 5)













2D TOPOGRAPHIC AMPLIFICATION

Due to topographic irregularities, amplitude of an incident wave can be severely amplified.

Consider the 2-D problem of indefinite, right wedge of a homogeneous and elastic material with S wave velocity β , and a harmonic SH wave incident along the direction of the axis of symmetry of the wedge and having the form:

$$v = v_0 \exp \left[i\omega(t + z/\beta)\right] = v_0 \exp \left(iKz\right) \exp \left(i\omega t\right)$$

Due to total reflection of the incident wave on the sides, at a generic point P of the wedge

interior, the total displacement consists of the sum of four contributions,

$$\begin{aligned} \mathbf{v} &= \mathbf{v}_0 \big[\exp(\mathrm{i} \mathbf{K} \mathbf{z}) + \exp(-\mathrm{i} \mathbf{K} \mathbf{z}) \big] & \textit{(vertically traveling waves)} \\ &+ \mathbf{v}_0 \big[\exp(\mathrm{i} \mathbf{K} \mathbf{x}) + \exp(-\mathrm{i} \mathbf{K} \mathbf{x}) \big] & \textit{(horizontally traveling waves)} \end{aligned}$$

and thus also
$$v = 2v_0(\cos Kx + \cos Kz)$$

(from Faccioli, 2005)













2D TOPOGRAPHIC AMPLIFICATION

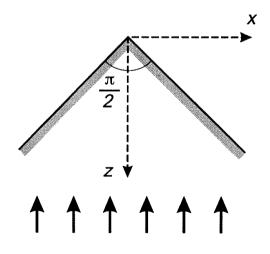
On the sides of the wedge, where $x = \pm z$, the displacement becomes:

$$v = 4v_0 \cos Kx = 4v_0 \cos Kz$$

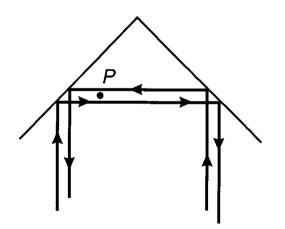
and on the apex (x = 0) $v(0,0) = 4v_0$

$$v(0,0) = 4v_0$$

This shows that the amplitude of the incident wave is quadruplicated at the wedge apex, independent of frequency. Amplitude is doubled w.r.t. that at the free surface of half-space.



$$v = v_o \exp [i\omega (t + \frac{z}{\beta})]$$



Sanchez-Sesma (1985)

$$v(x = 0, z = 0) = \frac{2\pi}{9}v_0$$

frequency independent and only for SH waves

(from Faccioli, 2005)





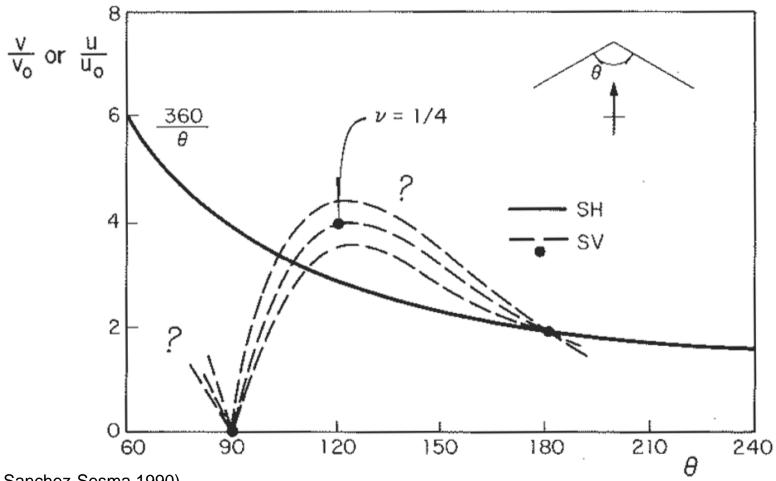


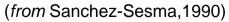






• 2D TOPOGRAPHIC AMPLIFICATION













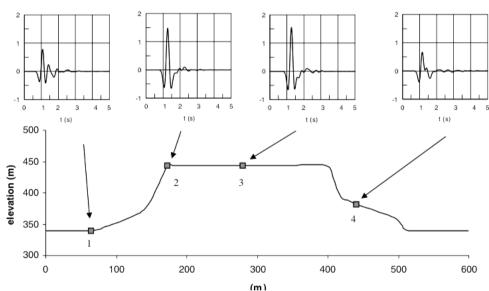




• 2D TOPOGRAPHIC AMPLIFICATION



Picture of Civita di Bagnoregio







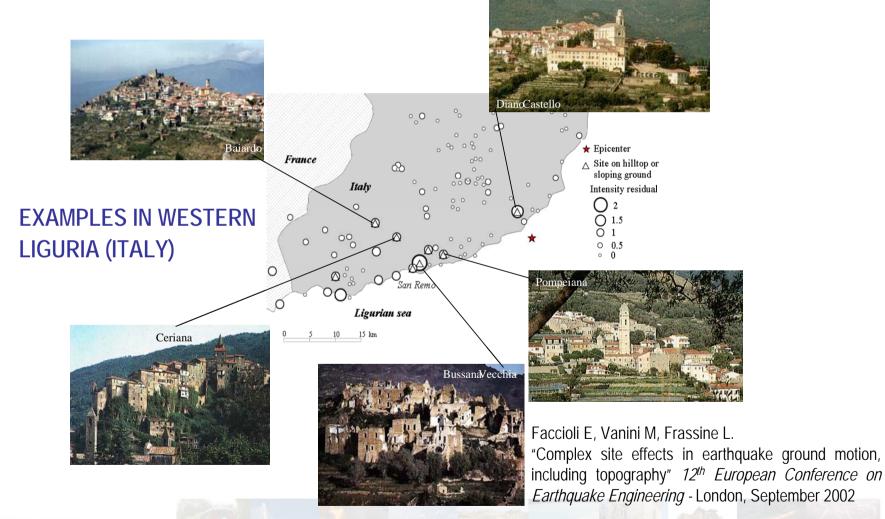








2D TOPOGRAPHIC AMPLIFICATION













Stochastic ground response analyses (further case study)





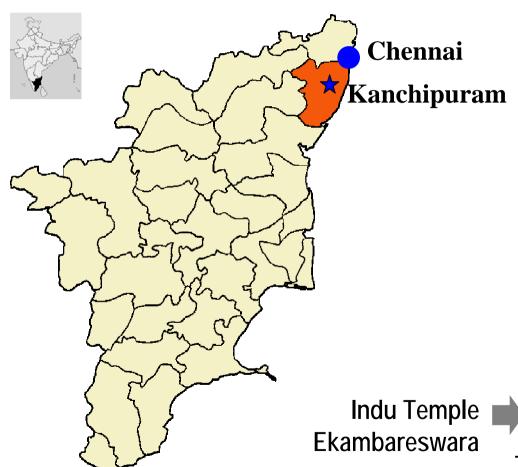




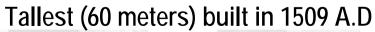




Archaeological site in Southern India:











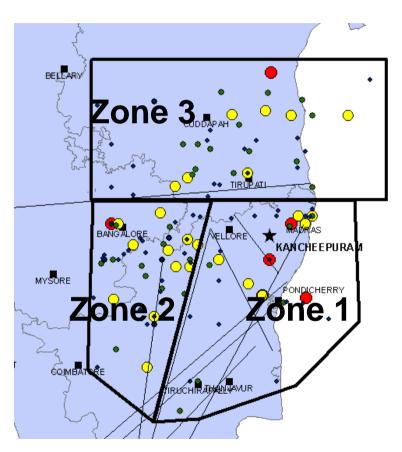




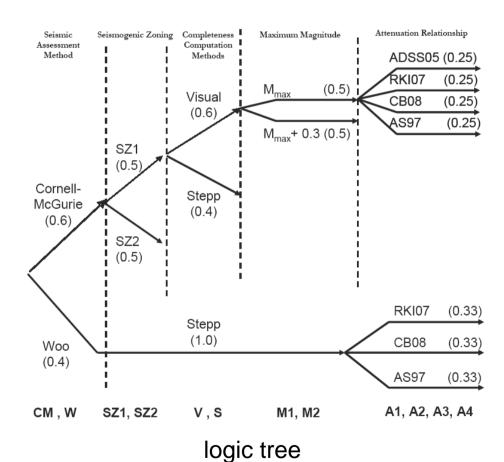




Probabilistic seismic hazard assessment:



seismogenic zoning







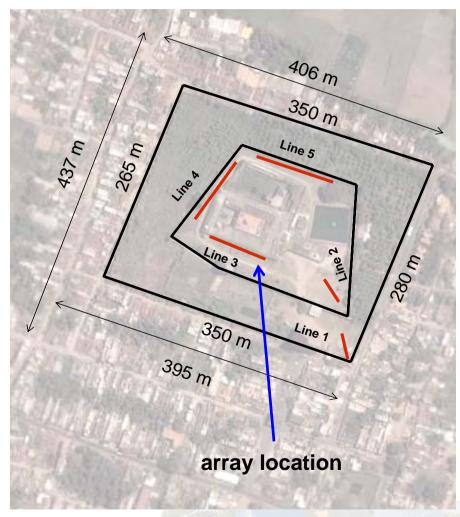






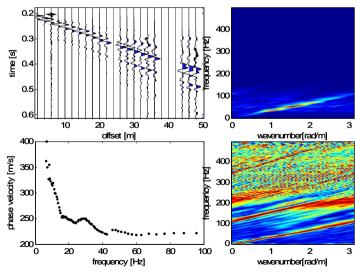


Geotechnical site characterization:



Two different types of geophysical seismic tests were performed (MASW and REMI) using the same experimental set-up.

The data for **MASW** and **REMI** tests was acquired using a linear array of vertical geophones.







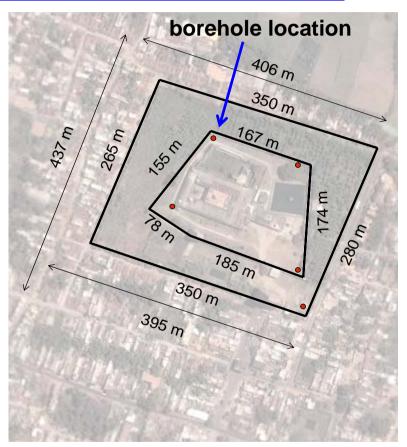




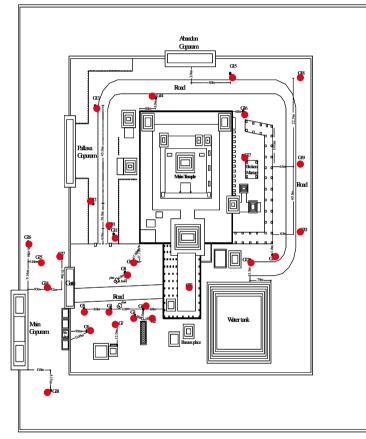




Geotechnical site characterization:



In order to identify the lithology at the site, five boreholes were excavated ranging from 10 to 20m in depth.



The **HVSR** technique was used as an effective tool to identify the natural frequency of the sites in order to see if there were large impedance contrast with the underlying bedrock.







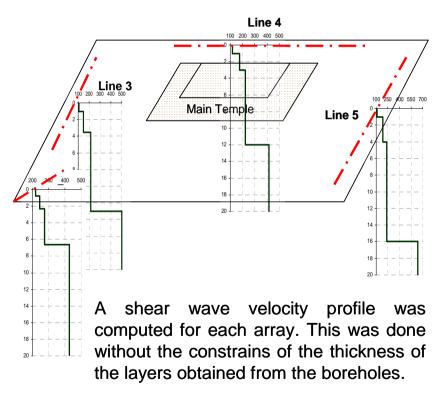


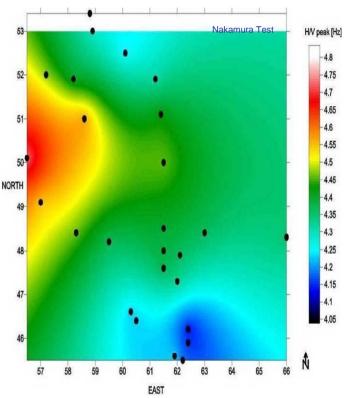




Geotechnical site characterization:

Shear Wave Velocity Profiles





From the Nakamura points test it can be seen that change in frequency is very small, thus the profile under the temple can be consider as a 1D.





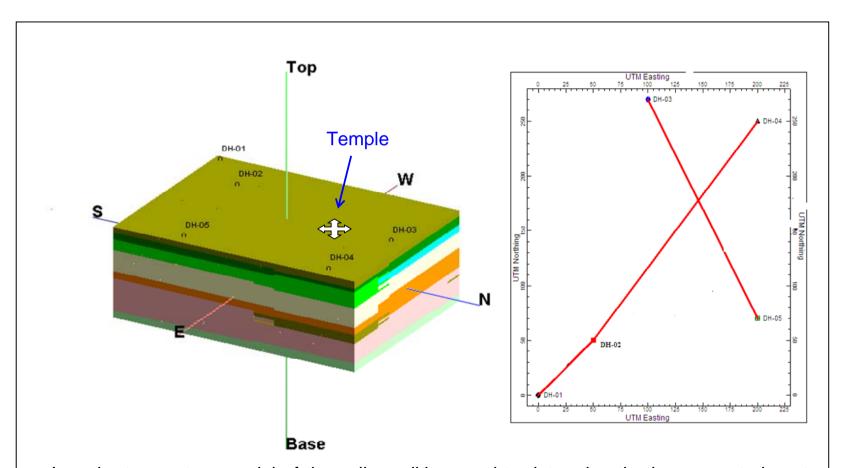


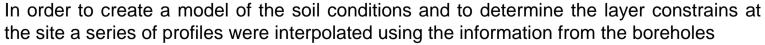






Geotechnical site modelling:











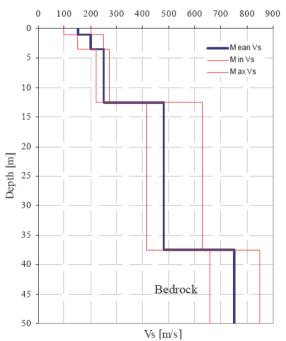






Stochastic site response analysis:

Layer	Thickness [m]	Uncertainty [%]	V _s [m/s]	Uncertainty [%]	$\rho [kN/m^3]$	Uncertainty [%]
1.	1.0	15	150	35	15	3
2.	2.5	25	200	40	16	5
3.	9.0	50	250	22	18	5
4.	25.0	68	480	38	19	5
5.	Bedrock	-	750	20	20	5





<u>Uncertainty</u> is defined as twice the standard deviation normalized by the mean value

- Uniform distribution was assumed for V_S and layer thicknesses for above range of variability.
- Analyses were conducted using Monte Carlo simulations associated with a sampling technique known as *Ipercube Latino*.
- A total of about 5,000 numerical seismograms were computed at the base of temple foundations.



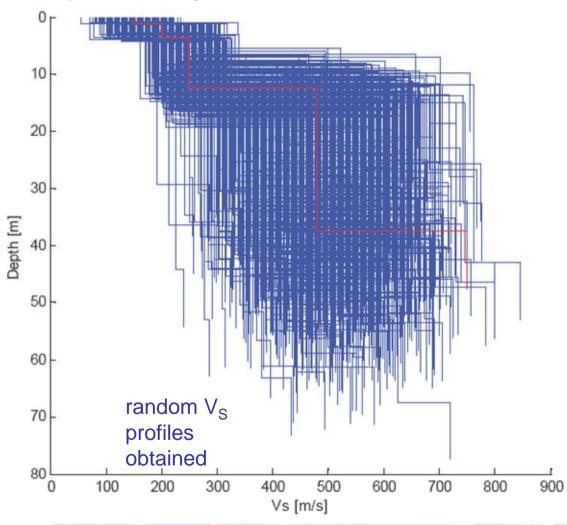


















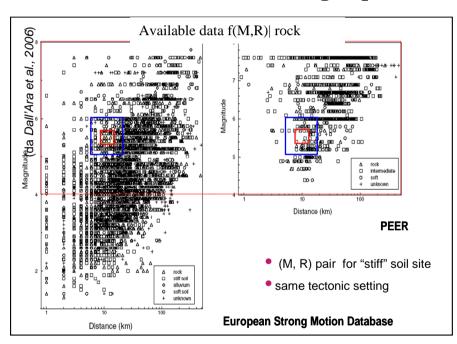






Stochastic site response analysis:

The selection of the best, spectrum-compatible group of accelerograms requires the fulfillment of each of the following steps:



Selection of a trial set of 7

Computation mean spectra

Determination of the deviation

Verification

A <-10%

Onerous procedures if carried out manually $\rightarrow \frac{n!}{(n-r)! \cdot r!}$ combination

→ Selection based on a Monte Carlo random automatic procedure (Dall'Ara et al., 2006)





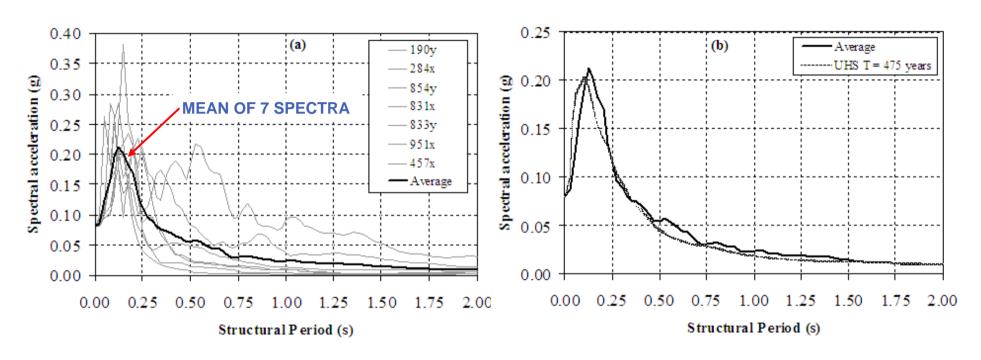








Stochastic site response analysis:



Spectrum-compatible input records for 475 return period (outcropping rock). PGA = 0.08 g

Seismic input plays an important role on the response. To take it into account, at every run an accelerogram is chosen <u>randomly</u> from a selected set of 7 real, spectrum-compatible records.



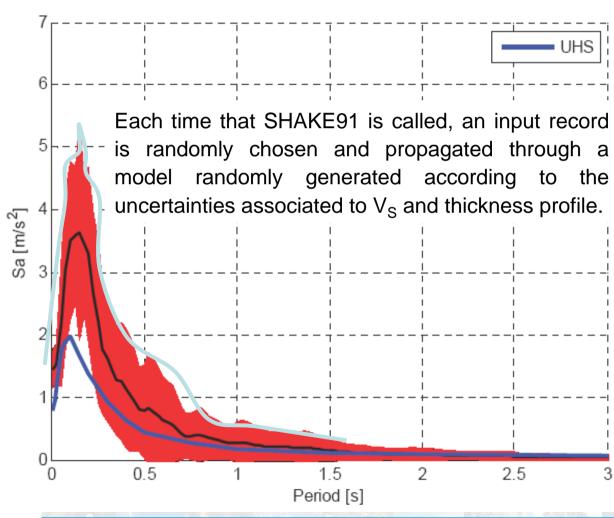














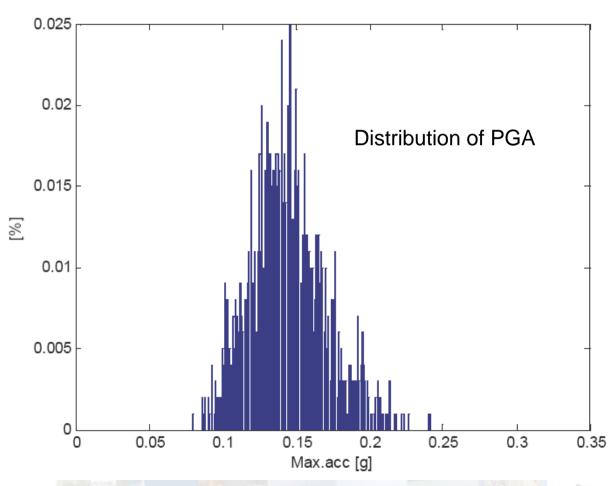














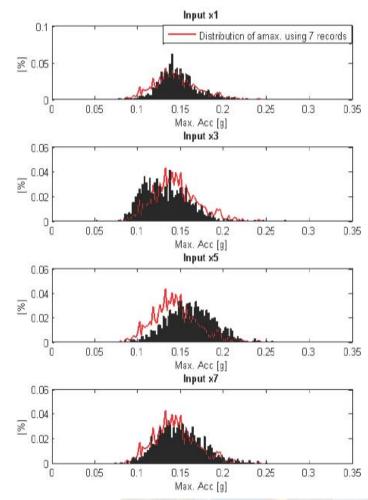


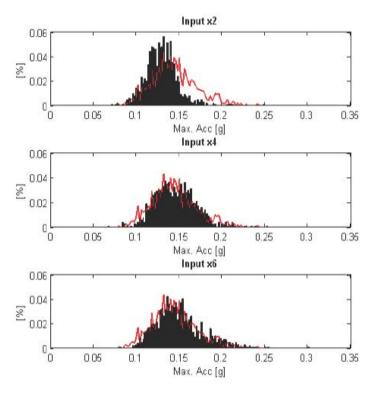












Distribution of PGA for individual records





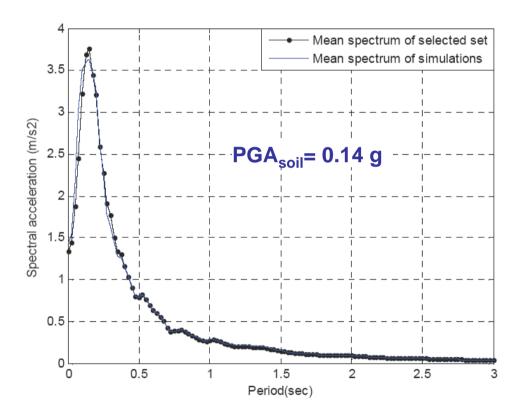








Stochastic site response analysis:



A set of 7 spectrum-compatible simulated records is selected using as a reference the mean spectrum at the free-surface. This is done to provide seismic input to carry out dynamic analyses of the temple considering the amplification due to site conditions.



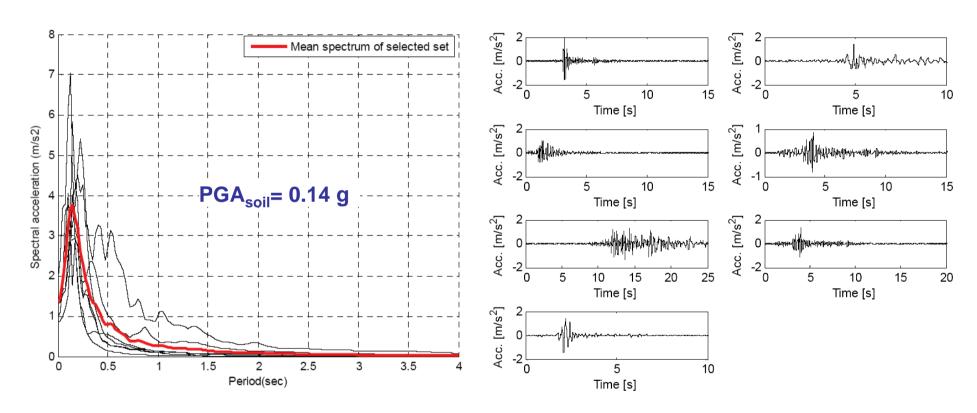












Set of 7 calculated records compatible with the mean spectrum obtained from stochastic simulations for the 475-year return period (free surface).



